Cellular/Molecular

The *Mef2c* Gene Dose-Dependently Controls Hippocampal Neurogenesis and the Expression of Autism-Like Behaviors

Sreetama Basu,[1] Eun Jeoung Ro,[1] Zhi Liu,[1] Hyunjung Kim,[2] Aubrey Bennett,[2] Seungwoo Kang,[2] and Hoonkyo Suh[1]
[1]Department of Neurosciences, Lerner Research Institute, Cleveland Clinic, Cleveland 44109, Ohio and [2]Department of Pharmacology & Toxicology, Medical College of Georgia, Augusta University, Augusta 30912, Georgia

Mutations in the activity-dependent transcription factor *MEF2C* have been associated with several neuropsychiatric disorders. Among these, autism spectrum disorder (ASD)-related behavioral deficits are manifested. Multiple animal models that harbor mutations in *Mef2c* have provided compelling evidence that *Mef2c* is indeed an ASD gene. However, studies in mice with germline or global brain knock-out of *Mef2c* are limited in their ability to identify the precise neural substrates and cell types that are required for the expression of *Mef2c*-mediated ASD behaviors. Given the role of hippocampal neurogenesis in cognitive and social behaviors, in this study we aimed to investigate the role of *Mef2c* in the structure and function of newly generated dentate granule cells (DGCs) in the postnatal hippocampus and to determine whether disrupted *Mef2c* function is responsible for manifesting ASD behaviors. Overexpression of *Mef2c* (*Mef2c^{OE}*) arrested the transition of neurogenesis at progenitor stages, as indicated by sustained expression of *Sox2^+* in *Mef2c^{OE}* DGCs. Conditional knock-out of *Mef2c* (*Mef2c^{cko}*) allowed neuronal commitment of *Mef2c^{cko}* cells; however, *Mef2c^{cko}* impaired not only dendritic arborization and spine formation but also synaptic transmission onto *Mef2c^{cko}* DGCs. Moreover, the abnormal structure and function of *Mef2c^{cko}* DGCs led to deficits in social interaction and social novelty recognition, which are key characteristics of ASD behaviors. Thus, our study revealed a dose-dependent requirement of *Mef2c* in the control of distinct steps of neurogenesis, as well as a critical cell-autonomous function of *Mef2c* in newborn DGCs in the expression of proper social behavior in both sexes.

Key words: abDGC; adult hippocampal neurogenesis; autism; *Mef2C*

Significance Statement

Autism spectrum disorder (ASD) is a neurodevelopmental disorder causing significant social, communication, and behavioral deficits in children worldwide. Genetic complexity and heterogeneity associated with ASD have hindered the field from establishing any precise cellular substrate associated with ASD. Recent studies have implicated hippocampal neurogenesis as one of the key players in social behavior and ASD-like behaviors. Here, using conditional deletion of transcriptional factor *Mef2c* in hippocampal newborn neurons or adult-born DGCs (abDGCs), we have demonstrated how *Mef2c* impacts behavior by regulating the structural development, physiology, and function of abDGCs. Our results revealed the essential role of *Mef2c* in neurogenesis and identified hippocampal neurogenesis as a neural substrate necessary for social behaviors.

Introduction

Autism spectrum disorder (ASD) is a family of neurodevelopmental disabilities that is characterized by social deficits, repetitive or stereotyped movements, and communication impairment.

According to the CDC, 1 in every 54 children in the United States is diagnosed with ASD, and the prevalence of ASD is 4.3 times higher in boys than in girls. Over the past three decades, the diagnosis of ASD has not significantly advanced, and no proven cures have been developed (Medavarapu et al., 2019), mainly because the precise mechanisms and neural substrates underlying ASD have not been fully established.

One major factor that has hindered the field from establishing the precise etiology of ASD is the genetic complexity and heterogeneity of autism. Hundreds of genes have been implicated in autism, and a wide range of severity has been associated with each genetic mutation (Ey et al., 2011). Recent genetic analyses have provided critical clues to unraveling a "unifying pathway" that links various autism genotypes to common autism phenotypes (Geschwind and Levitt, 2007; Parikshak et al., 2013); the

2 · J. Neurosci., January 31, 2024 · 44(5):e1058232023

majority of autism-associated genes control common aspects of neurobiology, namely, neuronal development, migration, and connectivity (Voineagu et al., 2011; Delorme et al., 2013). The implication is that impaired structural and functional development of neurons can lead to autism-specific cognitive and social impairments (Geschwind, 1965). *Mef2c* (myocyte enhancer factor 2c) falls into this category because children (Paciorkowski et al., 2013; Rocha et al., 2016) and animal models (Tu et al., 2017; Harrington et al., 2020) harboring *Mef2c* germline and/ or de novo mutations (Le Meur et al., 2010; Wan et al., 2021) show autistic behaviors as well as altered neuronal development. *Mef2c* is a transcription factor that belongs to the MADS (MCM1, agamous, deficiens, and serum) response factor box family of transcription factors (Dietrich, 2013; Rashid et al., 2014; Chen et al., 2017a), and its function has been identified as an activator or repressor in a context-dependent manner (Rashid et al., 2014; Di Giorgio et al., 2017; Sebastian et al., 2018; Pereira et al., 2020). Four *Mef2* isoforms, including *Mef2a*, *Mef2b*, *Mef2c*, and *Mef2d* have been identified, and they have distinct but partially overlapping temporal and spatial expression patterns in the developing and adult brain (Lyons et al., 1995; Dietrich, 2013). The functions of the *Mef2* family have been identified in the context of neuronal development and several neuropsychiatric disorders, including ASD (Lipton et al., 2009; Harrington et al., 2016; Zhang and Zhao, 2022). Among these, *MEF2C* haploinsufficiency is associated with global developmental and motor delay, seizures, repetitive behaviors, as well as social deficits, some of which are manifested in ASD (Barbosa et al., 2008; Lipton et al., 2009; Harrington et al., 2016; Chen et al., 2017a; Assali et al., 2019; Borlot et al., 2019; Moyses-Oliveira et al., 2020; Zhang and Zhao, 2022). Indeed, an association of *MEF2C* mutations with some patients who are diagnosed with ASD has been identified (Bourgeron, 2015; Wang et al., 2018). Several genetically engineered mice harboring *Mef2c* mutations have recapitulated ASD-related behaviors, further supporting that *Mef2c* is an ASD gene (Barbosa et al., 2008; Harrington et al., 2016, 2020; Tu et al., 2017). However, global or brain-wide mutations in *Mef2c* limit the ability to link precise neural substrates that transmit *Mef2* mutations to the presentation of ASD-related behaviors.

Recent studies have implicated hippocampal neurogenesis as one of the key players in social behavior and ASD-like behaviors (Rubin et al., 2014; Montagrin et al., 2018; Cope et al., 2020). The continuous production and integration of newborn neurons provides ample plasticity to the hippocampus, which is critical for cognitive function, emotional stability, addictive behaviors, and social behaviors (Eisch and Harburg, 2006; Sahay and Hen, 2007; Lagace et al., 2010; Castilla-Ortega et al., 2016; Anacker and Hen, 2017; Lee et al., 2019; Toda et al., 2019). Neurogenesis is a tightly regulated process (Suh et al., 2009), and a combination of both intrinsic programs and environmental factors determines not only the number of newborn neurons but also their structural and functional development and circuitry integration (Song et al., 2012, 2016; Gonçalves et al., 2016a; Oppenheim, 2019; Abbott and Nigussie, 2020). Disruption of any of these processes results in impaired cognition, emotion, and social behaviors, providing compelling evidence that hippocampal neurogenesis may be a key player in the manifestation of ASD-related behaviors (Guo et al., 2011; Stephenson et al., 2011; Amiri et al., 2012; Hussaini et al., 2014; Sun et al., 2019; Bicker et al., 2021; Haan et al., 2021). Given the expression of *Mef2c* in dentate granule cells (DGCs) and the role of *Mef2c* in synapse formation and elimination (Mao et al., 1999; Flavell et al.,

2006; Harrington et al., 2016; Cosgrove et al., 2021), we hypothesized that hippocampal neurogenesis may be a critical neural substrate that transmits *Mef2c* deficiency into the expression of ASD-related behaviors.

To test this hypothesis, we employed a retrovirus-mediated gene transfer method and transgenic mice that allowed us to specifically manipulate the *Mef2c* gene dose in adult-born DGCs (abDGCs) and investigated the role of *Mef2c* in structure, function, and behavior. This approach identified the dose-dependent role of *Mef2c* in the development of abDGCs. While a higher gene dose of *Mef2c* than normal arrested neurogenesis at $Sox2^+$ neuronal progenitors, *Mef2c* deficiency interfered with structural maturation and spine formation of abDGCs, which underlie decreased excitatory synaptic transmission to abDGCs. Most importantly, specific deletion of *Mef2c* in abDGCs resulted in sociability and social recognition deficits, which are hallmarks of ASD behavior. Thus, our results revealed the essential role of *Mef2c* in neurogenesis and identified hippocampal neurogenesis as a neural substrate necessary for social behaviors.

Materials and Methods

Animals
All experimental protocols were approved by the Institutional Animal Care and Use Committee of the Cleveland Clinic Foundation and Augusta University Medical College of Georgia. C57BL/6 (stock no. 000664), $Mef2c^{fl/fl}$ or $Mef2c^{tm1Jjs}$/J (stock No. 025556), Ai3 or B6.Cg-Gt(ROSA)$^{26Sortm3(CAG-EYFP)Hze}$/J (stock no. 007903), and $Ascl^{tm1.1(Cre/ETR2)Jejo}$/J (stock no. 012882) were purchased from Jackson Laboratory. These mice were used to breed in-house to generate double ($Ascl1$-CreER^{T2}; $Mef2c^{flox/flox}$ and $Ascl1$-CreER^{T2}; $Ai3^{+/+}$) and triple transgenic mice ($Ascl1$-CreER^{T2}; $Mef2c^{flox/flox}$/$Ai3^{+/+}$). The mice were kept in a 12 h light/dark cycle, with food and water available ad libitum. All experimental procedures occurred during the light phase using both sexes.

Experimental design
Retrovirus injection
To label hippocampal newborn neurons, mice were anesthetized with 100 mg/kg ketamine plus 10 mg/kg xylazine, and a reporter-expressing retrovirus [RV-CAG-RFP; 10^8 CFU/ml; RV-$Mef2c$-tPT2A-GFP (Addgene plasmid #111771) or RV-CAG -GFP-IRES-Cre 5–8 × 10^7 CFU/ml] was injected bilaterally into the hippocampus. The following coordinates relative to bregma were used: anterior to posterior (AP), −1.7 mm; medial to lateral (ML), ±1.4 mm; and dorsal to ventral (DV), −2.35 mm. One microliter of virus was injected into each site through a Hamilton syringe with a 33-gauge needle. The injection speed was 0.1 μl/min. The needle was retained in place for 5 min before retraction.

Tamoxifen injection
Tamoxifen (180 mg/kg, i.p., dissolved in a 1:10 mixture of ethanol and corn oil, MilliporeSigma) was administered to $Ascl1$-CreER^{T2}; $Mef2c^{fl/fl}$, $Mef2c^{fl/fl}$ mice (control littermates) and $Ascl1$-CreER^{T2}; $Ai3^{fl/fl}$ or $Ascl1$-CreER^{T2}; $Mef2c^{flox/flox}$/$Ai3^{fl/fl}$ mice for 3 consecutive days in order to induce cre-mediated recombination and deletion of *Mef2c* only from newborn neurons in $Ascl1$-CreER^{T2}; $Mef2c^{fl/fl}$ or $Ascl1$-CreER^{T2}; $Mef2c^{flox/flox}$/$Ai3^{fl/fl}$ mice when they were 6–8 weeks old.

Immunohistochemistry
The following antibodies were used in this study: GFAP (rabbit and/ guinea pig, Dako and Advanced Immuno; 1:1,000); SOX2 (goat, Santa Cruz Biotechnology, and rabbit, Chemicon 1:500); DCX (goat, Santa Cruz Biotechnology, 1:500); NEUROD1 (goat, Santa Cruz Biotechnology, 1: 200); MEF2C (rabbit, Abcam, and cell signaling, 1:1,000); PROX1 (rabbit, Chemicon, 1:500); TBR2 (rabbit, Abcam, 1:200); and NEUN (mouse, Chemicon, 1:1,000); secondary antibodies (AF555/AF647-donkey anti-goat, AF488/AF555/AF647-donkey

anti-rabbit, AF 488/AF 647-donkey anti-mouse, AF 488/AF 647-donkey anti-guinea pig) were purchased from Jackson ImmunoResearch. Briefly, animals were deeply anesthetized with a cocktail of ketamine (300 mg/kg) and xylazine (30 mg/kg) and transcardially perfused first with 0.9% saline and subsequently with 4% paraformaldehyde (PFA). Brains were dissected and postfixed overnight in PFA at 4°C. Brains were cryoprotected in 30% sucrose for 48 h at 4°C and sectioned at 40 µm with a sliding microtome (Leica SM2010 R). Floating tissue sections were washed 3 times in tris-buffered saline (TBS) and blocked in TBS-Tween (TBST) containing 3% donkey serum. Tissue was then incubated with primary antibodies (made in the same blocking solution) overnight at 4°C. Tissues were then washed 3 times for 15 min in TBST before incubation with secondary antibodies at 1:400 for 2 h. Tissues were then washed 3 times in TBST for 15 min. Finally, tissues were rinsed with PBS, counterstained with DAPI (Sigma-Aldrich, D9542), and mounted.

Morphological analysis
For quantification of MEF2C colocalization with different neurogenesis markers (Staging) and MEF2C overexpression (*Mef2c^OE*) experiments, images were taken at 40× with a zoom factor 3 using a Zeiss confocal microscope in three separate animals per experiment. For the MEF2C expression pattern in newborn neurons using retrovirus RV-CAG-RFP, 20× and 60× images were taken from three animals (30–50 cells quantified from each animal) at 2, 4, 8, and 12 weeks after virus injection (which corresponded to the ages of the newborn neurons). Dendritic length and spine analysis methods pertaining to studying the morphology of newborn neurons were described in detail previously (Lee et al., 2019). Briefly, for morphological analysis, z-series images at 1 µm intervals were captured for GFP-expressing neurons under a 40× oil objective using a Zeiss confocal microscope. Quantification and analysis were performed using ImageJ and software with the NeuronJ plugin for measurements of dendritic length. Sholl analysis was performed with a semi-manual method, where the concentric circles correlating to each branch point intersection were generated using ImageJ and Sholl plugin and the total number of intersections per 5 µm was counted manually. For analysis of dendritic spine density, z-series images with 0.1 µm intervals were captured under a 63× oil objective with a digital zoom factor of 4. The distal, middle, and proximal segments of the dendrite were captured, and the linear spine density was determined. The maximum z-projection images were opened in ImageJ software to measure the length of each segment. The number of spines on each segment was counted manually and is presented as the number of spines per micrometer. Spines were categorized into mushroom, thin, or stubby spines on the basis of three parameters, including spine length, diameter of the neck, and diameter of the spine head. Spines were scored as mushrooms if the diameter of the head was 3 times larger than that of the neck, as stubby spines if the diameter of the spine head was greater than the spine length, or as thin spines when the spine length was greater than the diameter of the head.

Brain slice preparation and ex vivo electrophysiology
Brain slices containing the hippocampus were prepared as described previously (Hong et al., 2019; Kang et al., 2020). Briefly, mice were deeply anesthetized using ketamine/xylazine (100 mg/10 mg/kg, i.p.), and the brain was rapidly removed and placed in ice-cold sucrose-based artificial cerebrospinal fluid (aCSF) containing the following (in mM): 75 sucrose, 87 NaCl, 2.5 KCl, 11.25 NaH$_2$PO$_4$, 7 MgCl$_2$, 0.5 CaCl$_2$, 25 NaHCO$_3$, 0.3 L-ascorbate, and 25 glucose, and oxygenated with 95% O$_2$/5% CO$_2$. Coronal (350 µm) slices were cut with a vibrating compresstome (VF-310-0Z, Precisionary Instruments), then transferred to a holding chamber, and incubated for 30 min at 34°C and kept for at least 1 h at room temperature (24–25°C) in carbonated (95% O$_2$/5% CO$_2$) standard artificial cerebrospinal fluid (aCSF) containing the following (in mM): 126 NaCl, 2.5 KCl, 1.25 NaH$_2$PO$_4$, 1 MgCl$_2$, 2 CaCl$_2$, 25 NaHCO$_3$, and 11 glucose. After equilibration, a single slice was transferred to a submersion-type recording chamber and mechanically stabilized with an anchor (Warner Instruments, Hamden, CT). Electrical signals were recorded with an Axon 700B amplifier, a Digidata 1550B A/D converter, and Clampfit 11.0 software (Molecular Devices). Throughout the experiments, the bath was continually perfused with warm (32°C) carbonated aCSF (2.0–2.5 ml/min). Patch pipettes had a resistance of 4–6 MΩ when filled with a solution containing (in mM): 140 Cs-methanesulfonate, 5 KCl, 2 MgCl$_2$, 10 HEPES, 2 MgATP, and 0.2 Na2GTP for voltage clamping. The pH was adjusted to 7.2 with Tris-base and the osmolality to 310 mOsmol/L with sucrose. The newborn neurons were identified by the expression of GFP fluorescence. mEPSCs and mIPSCs were recorded in the presence of tetrodotoxin (0.5 µM) at a holding potential of −70 and 0 mV, respectively. The EPSCs were confirmed pharmacologically with the AMPA receptor antagonist DNQX (20 µM) and the NMDA receptor antagonist AP5 (50 µM). The IPSCs were confirmed with the GABA$_A$ receptor antagonist Picrotoxin (PTX, 100 µM).

Behavioral protocols
All behavioral tests were performed in the Rodent Behavioral Core of the Cleveland Clinic during the animal's light cycle phase. Age-matched littermates, using both male and female sexes, at 14–18 weeks of age were used for these studies as controls. All behavioral tests were performed 8–12 weeks after tamoxifen injection for two separate cohorts, except for the open field and fear conditioning, which were done only at the 12-week time point. Each behavioral paradigm was separated by a day. All home cages containing mice were transported to the testing room at least 30 min prior to the start of testing. The tests were scored using Ethovision software.

Three-chamber social interaction. This test comprised a three-chamber white opaque box with openings for the mice to pass through each chamber. The center region length was 22.5 cm, the two sides measured 18.5 cm each, and the two side chambers had two empty pencil cup holders. Each test consisted of 30 min. The first 10 min was for habituation where each experimental mouse when placed inside the center explored all three chambers for 10 min. After 10 min, the mice were taken out and placed in a cage, during which one novel mouse that the experimental mouse had never interacted with before (stimulant mouse 1) was placed inside the pen holder on one side, while a Lego object was placed on the other side's pen holder. The experimental mouse was allowed to explore for 10 min, after which it was returned to the cage again. Then, the Lego was replaced by another novel mouse (stimulant mouse 2), and the experimental mouse was again placed in the center of the three-chamber box and explored the chambers for 10 more minutes. After 10 min, the experimental mice were taken out and placed back in their home cage. The chambers and the pen holders were thoroughly cleaned with trifectant between each experiment. The object and the mice were alternately switched between each experimental mouse so as to remove potential bias from behavior.

Fear conditioning. Mice were initially exposed to a neutral context with metal grid floors for a 3 min habituation period, followed by the presentation of a 30 s tone (conditioned stimulus CS; 90 dB white noise) that co-terminated with a 2 s 1.2 mA footshock (unconditioned stimulus; UCS). Following the shock, the rodent was given a 2 min inter-trial interval before receiving a second tone and footshock pairing, followed by a 2 min post-shock "recovery" period. Freezing was recorded using freeze frame software. Chambers were cleaned with trifectant between each experiment. For the contextual memory test, 24 h later the mice were exposed to the same context for 5 min, without the tone or shock. Three hours later, cued fear memory was tested by placing the mice in a completely different context than the training day (different floor; white plastic and vanilla odor) for 6 min. The first 3 min were for habituating to the novel environment, followed by 3 min of constant presentation of the control stimulus (white noise).

Open field test. During this test, mice were first placed (from one corner) inside a white opaque square box, 45 cm in width and height, and allowed to explore for 10 min. For the analysis, the white square box was divided into 26 zones, each approximately 9 cm in diameter. The

Table 1. Descriptive statistics

Figure #	Experiment	Animal (N) and/cell number (n)	Statistics performed	p value	t	Degrees of freedom and/$F_{(DFn, DFd)}$	SE of difference and/95.00% CI of diff.
1C	MEF2C deletion with retrovirus	$n = 10$	Unpaired t test	<0.0001	62.61	Degrees of freedom = 18	−84.23 to −78.77 (95% CI of difference)
2E left	% colocalization with SOX2 2 WPI	$N = 3$, $n = 15$	Unpaired t test	<0.000001	78.51	Degrees of freedom = 28	0.9595 (SE of difference)
	% colocalization with SOX2 4 WPI	$N = 3$, $n = 15$	Unpaired t test	<0.000001	75.22	Degrees of freedom = 28	1.241(SE of difference)
	% colocalization with SOX2 8 WPI	$N = 3$, $n = 15$	Unpaired t test	<0.000001	107	Degrees of freedom = 28	0.819 (SE of difference)
2E middle	% colocalization with TBR2 2 WPI	$N = 3$, $n = 15$	Unpaired t test	<0.000001	47.62	Degrees of freedom = 28	0.3780 (SE of difference)
2E right	% colocalization with PROX1 2 WPI	$N = 3$, $n = 15$	Unpaired t test	<0.000001	119.3	Degrees of freedom = 28	0.7015 (SE of difference)
	% colocalization with PROX1 4 WPI	$N = 3$, $n = 15$	Unpaired t test	<0.000001	129.1	Degrees of freedom = 28	0.7551 (SE of difference)
	% colocalization with PROX1 8 WPI	$N = 3$, $n = 15$	Unpaired t test	<0.000001	394.2	Degrees of freedom = 28	0.252 (SE of difference)
2E far right	% colocalization with NEUN 2 WPI	$N = 3$, $n = 15$	Unpaired t test	<0.000001	99.57	Degrees of freedom = 28	0.8496 (SE of difference)
	% colocalization withNEUN 4 WPI	$N = 3$, $n = 15$	Unpaired t test	<0.000001	177.8	Degrees of freedom = 28	0.5492(SE of difference)
	% colocalization with NEUN 8 WPI	$N = 3$, $n = 15$	Unpaired t test	<0.000001	394.2	Degrees of freedom = 28	0.252 (SE of difference)
3C left	Total length 4 WPI	$N = 3$; $n = 13$	Unpaired t test	0.0149	2.624	Degrees of freedom = 24	−198.7 to −23.72 (95% CI of diff.)
3E left	Total length 8 WPI	$N = 3$; $n = 17$	Unpaired t test	0.0008	3.713	Degrees of freedom = 32	−174.0 to −50.72 (95% CI of diff.)
3G left	Total length 12 WPI	$N = 3$; $n = 16$	Unpaired t test	<0.0001	6.88	Degrees of freedom = 30	−306.6 to −166.2 (95% CI of diff.)
3C right	Sholl analysis 4 WPI	$N = 3$; $n = 9$	Two-way ANOVA				
			Interaction	<0.0001		$F_{(25, 390)} = 4.531$	0.09956 (SE of difference)
			Distance from soma	<0.0001		$F_{(25, 390)} = 11.44$	
			Genotype	<0.0001		$F_{(1, 390)} = 164.7$	
3E right	Sholl analysis 8 WPI	$N = 3$; $n = 13$	Two-way ANOVA				
			Interaction	<0.0001		$F_{(25, 624)} = 5.625$	0.1026 (SE of difference)
			Distance from soma	<0.0001		$F_{(25, 624)} = 15.14$	
			Genotype	<0.0001		$F_{(1, 624)} = 267.4$	
3G right	Sholl analysis 12 WPI	$N = 3$; $n = 9$	Two-way ANOVA				
			Interaction	<0.0001		$F_{(25, 338)} = 6.346$	0.1337 (SE of difference)
			Distance from soma	<0.0001		$F_{(25, 338)} = 9.012$	
			Genotype	<0.0001		$F_{(1, 338)} = 140.5$	
3I	Spine density 4 WPI	$N = 3$; $n = 28$	Multiple unpaired t test				
			Inner	0.060278	1.919	Degrees of freedom = 54	0.111 (SE of difference)
			Middle	0.221362	1.237	Degrees of freedom = 54	0.1049 (SE of difference)
			Outer	0.654163	0.4506	Degrees of freedom = 52	0.1046 (SE of difference)
3K	Spine density 8 WPI	$N = 3$; $n = 24$	Multiple unpaired t test				
			Inner	<0.000001	6.169	Degrees of freedom = 44	0.09342 (SE of difference)
			Middle	<0.000001	7.494	Degrees of freedom = 46	0.09112 (SE of difference)
			Outer	<0.000001	6.305	Degrees of freedom = 45	0.1022 (SE of difference)
3M	Spine density 12 WPI	$N = 3$; $n = 24$	Multiple unpaired t test				
			Inner	0.004434	3.021	Degrees of freedom = 39	0.1654 (SE of difference)
			Middle	0.006856	2.841	Degrees of freedom = 43	0.1263 (SE of difference)
			Outer	0.006796	2.851	Degrees of freedom = 41	0.1732 (SE of difference)
3O left	Spine morphology of inner dendrite segment (4 WPI)	$N = 3$; $n = 8$	Multiple unpaired t test: inner				
			Mushroom	0.00265	3.645	Degrees of freedom = 14	0.05967 (SE of difference)
			Thin	0.010468	2.988	Degrees of freedom = 13	0.1894 (SE of difference)
			Stubby	0.263911	1.164	Degrees of freedom = 14	0.0537 (SE of difference)
3O middle	Spine morphology of middle dendrite segment (4 WPI)	$N = 3$; $n = 8$	Multiple unpaired t test: middle				
			Mushroom	0.000003	7.754	Degrees of freedom = 13	0.04076 (SE of difference)
			Thin	0.024526	2.543	Degrees of freedom = 13	0.1644 (SE of difference)
			Stubby	0.582157	0.5643	Degrees of freedom = 13	0.3702 (SE of difference)

(*Table continues.*)

Table 1. Continued

Figure #	Experiment	Animal (N) and cell number (n)	Statistics performed	p value	t	Degrees of freedom and/$F_{(DFn, DFd)}$	SE of difference and/95.00% CI of diff.
3O right	Spine morphology of outer dendrite segment (4 WPI)	$N = 3$; $n = 8$	Multiple unpaired t test: outer				
			Mushroom	0.011125	2.997	Degrees of freedom = 12	0.06864 (SE of difference)
			Thin	0.060714	2.07	Degrees of freedom = 12	0.1622 (SE of difference)
			Stubby	0.519811	0.6631	Degrees of freedom = 12	0.04524 (SE of difference)
3P left	Spine morphology of inner dendrite segment (8 WPI)	$N = 3$; $n = 12$	Multiple unpaired t test: inner				
			Mushroom	0.10352	1.698	Degrees of freedom = 22	0.03901 (SE of difference)
			Thin	0.000002	6.417	Degrees of freedom = 22	0.1616 (SE of difference)
			Stubby	0.831961	0.2147	Degrees of freedom = 22	0.03978 (SE of difference)
3P middle	Spine morphology of middle dendrite segment (8 WPI)	$N = 3$; $n = 12$	Multiple unpaired t test: middle				
			Mushroom	0.264056	1.146	Degrees of freedom = 22	0.04526 (SE of difference)
			Thin	0.000002	6.403	Degrees of freedom = 22	0.1167 (SE of difference)
			Stubby	0.576916	0.5663	Degrees of freedom = 22	0.04194 (SE of difference)
3P right	Spine morphology of outer dendrite segment (8 WPI)	$N = 3$; $n = 12$	Multiple unpaired t test: outer				
			Mushroom	0.947386	0.06675	Degrees of freedom = 22	0.03745 (SE of difference)
			Thin	0.003662	3.251	Degrees of freedom = 22	0.1425 (SE of difference)
			Stubby	0.337423	0.9807	Degrees of freedom = 22	0.03917 (SE of difference)
3Q left	Spine morphology of inner dendrite segment (12 WPI)	$N = 3$; $n = 12$	Multiple unpaired t test: inner				
			Mushroom	0.001538	3.861	Degrees of freedom = 15	0.07033 (SE of difference)
			Thin	0.000018	6.163	Degrees of freedom = 15	0.1877 (SE of difference)
			Stubby	0.121028	1.644	Degrees of freedom = 15	0.04554 (SE of difference)
3Q middle	Spine morphology of middle dendrite segment (12 WPI)	$N = 3$; $n = 12$	Multiple unpaired t test: middle				
			Mushroom	0.057134	2.025	Degrees of freedom = 19	0.07824 (SE of difference)
			Thin	0.009441	2.887	Degrees of freedom = 19	0.2566 (SE of difference)
			Stubby	0.209734	1.298	Degrees of freedom = 19	0.04145 (SE of difference)
3Q right	Spine morphology of outer dendrite segment (12 WPI)	$N = 3$; $n = 12$	Multiple unpaired t test: outer				
			Mushroom	0.787481	0.2726	Degrees of freedom = 24	0.0655 (SE of difference)
			Thin	0.019689	2.499	Degrees of freedom = 24	0.23 (SE of difference)
			Stubby	0.377216	0.8997	Degrees of freedom = 24	0.04247 (SE of difference)
4E	mEPSC amplitude	$N = 6$, $n = 9$	Unpaired t test	0.3532	0.9561	Degrees of freedom = 16	−1.658 to 4.381 (95% CI of diff.)
	mEPSC frequency	$N = 6$, $n = 9$	Unpaired t test	0.0182	2.629	Degrees of freedom = 16	−1.378 to −0.1476 (95% CI of diff.)
4G	mIPSC amplitude	$N = 6$, $n = 9$–10	Unpaired ttest	0.9341	0.08388	Degrees of freedom = 17	−4.226 to 4.576 (95% CI of diff.)
	mIPSC frequency	$N = 6$, $n = 9$–10	Unpaired t test	0.646	0.4676	Degrees of freedom = 17	−1.107 to 0.7057 (95% CI of diff.)
5J	Contextual fear conditioning	$N = 16$–17	Unpaired t test	0.0091	2.801	Degrees of freedom = 28	−34.80 to −5.403 (95% CI of diff.)
5D	Three-chamber social interaction: habituation phase	$N = 22$, 21	Two-way ANOVA multiple comparison				
			Tukey's multiple comparison: control (Side1 vs Side2)	0.3891			−22.20 to 77.53 (95% CI of diff.)
			MEF2CcKO (Side1 vs Side2)	0.8904			−40.21 to 59.52 (95% CI of diff.)
			Interaction	$p = 0.5291$		$F_{(2, 126)} = 0.6399$	
			Movement	$p < 0.0001$		$F_{(2, 126)} = 26.55$	
			Genotype	$p = 0.5893$		$F_{(1, 126)} = 0.2930$	

(Table continues.)

Table 1. Continued

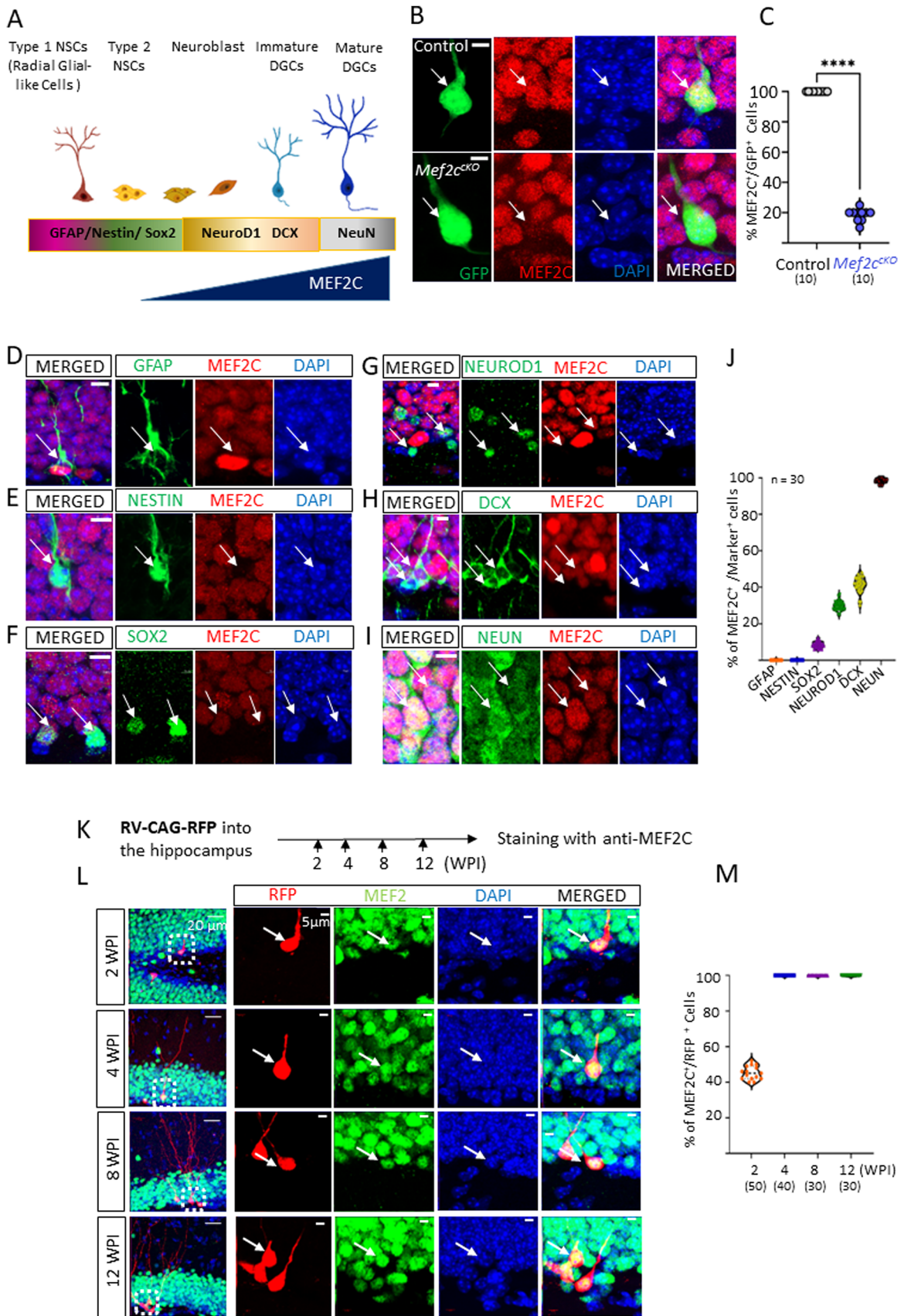| Figure #	Experiment	Animal (N) and/cell number (n)	Statistics performed	p value	t	Degrees of freedom and $F_{(DFn, DFd)}$	SE of difference and 95.00% CI of diff.
5F	Three-chamber social interaction: sociability phase	$N = 22, 21$	Two-way ANOVA multiple comparison: uncorrected fishers LSD				
			Control (object vs mice)	0.0009	3.431	DF = 82	−151.3 to −40.26 (95% CI of difference)
			MEF2CcKO (object vs mice)	0.4884	0.696	DF = 82	−73.24 to 35.28 (95% CI of diff.)
			Interaction	0.0524		$F_{(1, 82)} = 3.873$, DF = 1	
			Row factor	0.0043		$F_{(1, 82)} = 8.648$, DF = 1	
			Column factor	0.9131		$F_{(1, 82)} = 0.01199$, DF = 1	
5H	Three-chamber social interaction: social novelty phase	$N = 22, 21$	Two-way ANOVA multiple comparison: uncorrected fishers LSD				
			Control (familiar vs novel)	0.0012	3.356	DF = 82	−150.1 to −38.37
			MEF2CcKO (familiar vs novel)	0.2811	1.085	DF = 82	−88.35 to 25.98
			Interaction	0.1204		$F_{(1, 82)} = 2.462$, DF = 1	
			Social novelty	0.0025		$F_{(1, 82)} = 9.744$, DF = 1	
			Genotype	0.7971		$F_{(1, 82)} = 0.06652$, DF = 1	
5I	Contextual fear conditioning	$N = 15$	Unpaired t test	0.0091	2.801	Degrees of freedom = 28	−34.80 to −5.403
5K	Cued fear conditioning	$N = 15$	Two-way ANOVA multiple comparison				
			Control	<0.0001	12.99	DF = 58	−80.32 to −56.19 (95% CI of diff.)
			MEF2CcKO	<0.0001	11.69	DF = 58	−71.16 to −47.80 (95% CI of diff.)
5M	Novel object recognition	$N = 20$	Two-way ANOVA multiple comparison uncorrected fishers LSD				
			Control	0.0003	3.747	DF = 76	−7.767 to −2.376 (95% CI of diff.)
			MEF2CcKO	0.0031	3.058	DF = 76	−6.835 to −1.444 (95% CI of diff.)
			Interaction	$p = 0.6275$		$F_{(1, 76)} = 0.2374$, DF = 1	
			Row factor	$p < 0.0001$		$F_{(1, 76)} = 23.16$, DF = 1	
			Column factor	$p = 0.4127$		$F_{(1, 76)} = 0.6785$, DF = 1	
5N	Novel object recognition: distance moved	$N = 19, 17$	Unpaired t test	0.1662	1.419	Degrees of freedom = 30	−662.3 to 119.3
5P	Open field	$N = 19, 17$	Two-way ANOVA multiple comparison: uncorrected fishers LSD				
			Control (center vs periphery)	<0.0001	15.11	DF = 58	−423.8 to −324.6 (95% CI of diff.)
			MEF2CcKO (center vs periphery)	<0.0001	16.53	DF = 58	−444.4 to −348.4 (95% CI of diff.)
			Interaction	$p = 0.5227$		$F_{(1, 58)} = 0.4135$, DF = 1	
			Center vs periphery	$p < 0.0001$		$F_{(1, 58)} = 499.5$, DF = 1	
			Genotype	$p = 0.9674$		$F_{(1, 58)} = 0.001681$, DF = 1	
5Q	Open field: distance moved	$N = 19, 17$	Unpaired t test	0.3597	0.9302	Degrees of freedom = 30	−450.5 to 1,204

Figure 1. Continued.

exploration time in the outer 16 zones was considered as the periphery, while the inner 10 zones were considered as the time spent in the center.

Novel object recognition test. This test was comprised of the same white opaque box used in the open field test, where two similar objects were first placed at two corners (glass bottle with bedding), and the mice were allowed to explore this arena with the objects freely for 5 min; this was the habituation phase (each time the experimental mice were placed inside the box from a particular corner away from the two objects). After 1 h, they were again placed back into the same arena with the same objects for 5 min; this was the familiarization phase. Four hours after the habituation and familiarization phases, one of the objects was replaced by a novel object (Lego), and the mice were allowed to explore the arena with the familiar and the new object for 10 min. Each time, the side for the familiar object (bottle with glass bedding) and the novel object (Lego) were exchanged alternately so as to remove potential bias.

Statistics
All statistical analyses were performed using commercial software (GraphPad Prism). Data were analyzed either by Student's t test or by two-way ANOVAs. Bonferroni's multiple comparison *post hoc* test was applied to compare differences among groups. The significance threshold was placed at $\alpha = 0.05$, and corrections for multiple comparisons are reflected in p values. Detailed descriptive statistics are presented in Table 1.

Results
MEF2C is expressed in DGCs, but not in neural stem cells
Neural stem/progenitor cells (NSCs) continuously produce new cells. Newly generated cells transit multiple stages and become DGCs that are integrated into existing hippocampal neural circuits (Suh et al., 2009; Song et al., 2016; Gage, 2019). To understand the temporal expression pattern of MEF2C, we used cell type-specific markers to define the developmental stages that express MEF2C during neurogenesis (Fig. 1A). *Mef2c* was deleted in DGCs by injecting a CRE-expressing retrovirus into the dentate gyrus (DG) of the hippocampus of *Mef2c*$^{fl/fl}$ mice, and the specificity of MEF2C antibody was confirmed by showing a significant reduction in MEF2C expression in *Mef2c*-deficient DGCs (Fig. 1B,C). Type 1 NSCs show a characteristic radial morphology and express GFAP or NESTIN in their radial processes (Suh et al., 2007, 2009; Song et al., 2016). MEF2C was not expressed in radial glial-like GFAP$^+$ cells (Fig. 1D) or GFP$^+$ cells in *Nestin-GFP* transgenic mice in which GFP is expressed under the control of NSC-specific promoter *Nestin* (Mignone et al., 2004) (Fig. 1E). However, the expression of MEF2C was initially detected in a subset of SOX2$^+$ Type 2 cells (Suh et al., 2007; Fig. 1F), as well as 40–50% of NEUROD1$^+$ or DCX$^+$ cells that represent neuroblasts or immature neurons (Fig. 1G,H). In the DG, 100% of NEUN$^+$ cells co-expressed MEF2C (Fig. 1I). Collectively, these results show that MEF2C expression is initiated at the later stage of SOX2$^+$ Type 2 progenitors, gradually increases in neuroblasts (NEUROD1$^+$) and immature neurons (DCX$^+$), and is sustained in fully differentiated DGCs (Fig. 1J).

To assess the expression of MEF2C during the differentiation of newborn cells into DGCs, we labeled newborn cells using a replication-incompetent retrovirus (RV) expressing a red fluorescent protein (RFP) and examined the expression of MEF2C during a time course of neuronal development of newborn cells (Fig. 1K). Because an RV only infects proliferating cells, we defined the time between the RV injection and examination as the maximal age of newborn cells. This age-synchronized labeling method revealed that almost 50% of 2-week-old abDGCs (RFP$^+$) were colocalized with MEF2C; however, 100% of mature abDGCs older than 4 weeks expressed MEF2C (Fig. 1L,M). Thus, MEF2C was expressed in neuronally committed cells and mature DGCs, consistent with the results from MEF2C immunohistochemistry with cell type-specific markers.

Mef2C overexpression arrests neuronal differentiation
To understand the gain-of-function effects of MEF2C on the development of newborn neurons, we overexpressed *Mef2c* (*Mef2c*^{OE}) in newborn neurons using RV-mediated gene delivery. The RV used was RV-*Mef2c*-tPT2A-GFP, which expresses both MEF2C and a green fluorescent protein (GFP) reporter gene (Liu et al., 2017). This RV was injected into the DG to overexpress MEF2C in abDGCs, and the effects of *Mef2c*^{OE} were compared to control mice that received a RFP- or GFP-expressing RV (RV-GFP or RV-RFP, pseudo-colored to green in the representative image) at 2, 4, and 8 weeks postinjection (WPI) (Fig. 2A). While only a small population of *Mef2c*^{OE} newborn cells maintained the typical morphology of DGCs with radially developed dendrites, the majority of *Mef2c*^{OE} newborn cells displayed abnormal structural development (Fig. 2B,C). *Mef2c*^{OE} newborn cells were clustered and failed to project their processes into the molecular layer, instead projecting processes either parallel to the granular layer or into the hilus, which is reminiscent of the morphology of immature stages of newborn cells (referred to as "projection" impairment; Fig. 2B,C). Moreover, some *Mef2c*^{OE} newborn cells migrated to the hilus instead of the granular layer (referred to as "migration" impairment; Fig. 2B,C). The onset of both projection and migration impairments in *Mef2c*^{OE} newborn cells was at 2 WPI, and such morphological deficits were sustained up to 8 weeks from birth, which is the longest time period that we examined (Fig. 2B,C).

To define the cell types of *Mef2c*^{OE} newborn cells, neuronal developmental stage-specific markers were used. A small population of *Mef2c*^{OE} cells that appeared to develop normally showed colocalization with PROX1, a marker for DGCs (Fig. 2D). Surprisingly, *Mef2c*^{OE} cells with structural and migratory impairments were predominantly colocalized with SOX2, but not with any other cell type-specific markers, including GFAP, Tbr2, NEUN, or PROX1 (which represent astrocytes, immature and mature neurons, respectively; Fig. 2D,E). SOX2 co-expression

---

←

Figure 1. MEF2C is mainly expressed in DGCs, but not in neural stem cells. *A*, Cartoon illustrating the progression of neurogenesis and the temporal expression of corresponding stage-specific markers. *B,C*, RV-CAG-GFP-IRES-Cre injection into *Mef2c*$^{flox/flox}$ mice deleted *Mef2c* in ∼80% of infected (GFP$^+$) abDGCs. *D,E*, Immunohistochemistry with neural stem cell (NSC) markers showed that MEF2C is not expressed in GFAP$^+$ or *Nestin*$^+$ radial glial-like cells. *F–H*, A subset of SOX2$^+$, NEUROD1$^+$, and DCX$^+$ cells showed colocalization with MEF2C. *I*, MEF2C was expressed in 100% of NEUN$^+$ DGCs. *D–I*, MEF2C, stage-specific markers, and DAPI counterstaining are shown in green, red, and blue, respectively. Arrows indicate the location of stage-specific markers. *J*, Percentage of MEF2C$^+$ cells among stage-specific markers shown in *A–F*. For each cell stage marker, 30 cells from three mice were examined. *K*, Experimental paradigm to determine the temporal expression of MEF2C during neurogenesis. *L,M*, Retrovirus-mediated cell birth date labeling showed that MEF2C expression (green) was detected in approximately 50% of 2-week-old abDGCs (red) and was sustained in 100% of abDGCs older than 4 weeks. RFP$^+$ cells ($n = 30–50$) from three mice were examined for colocalization with MEF2C. Numbers in parentheses represent cell numbers. The scale bar is 5 μm.
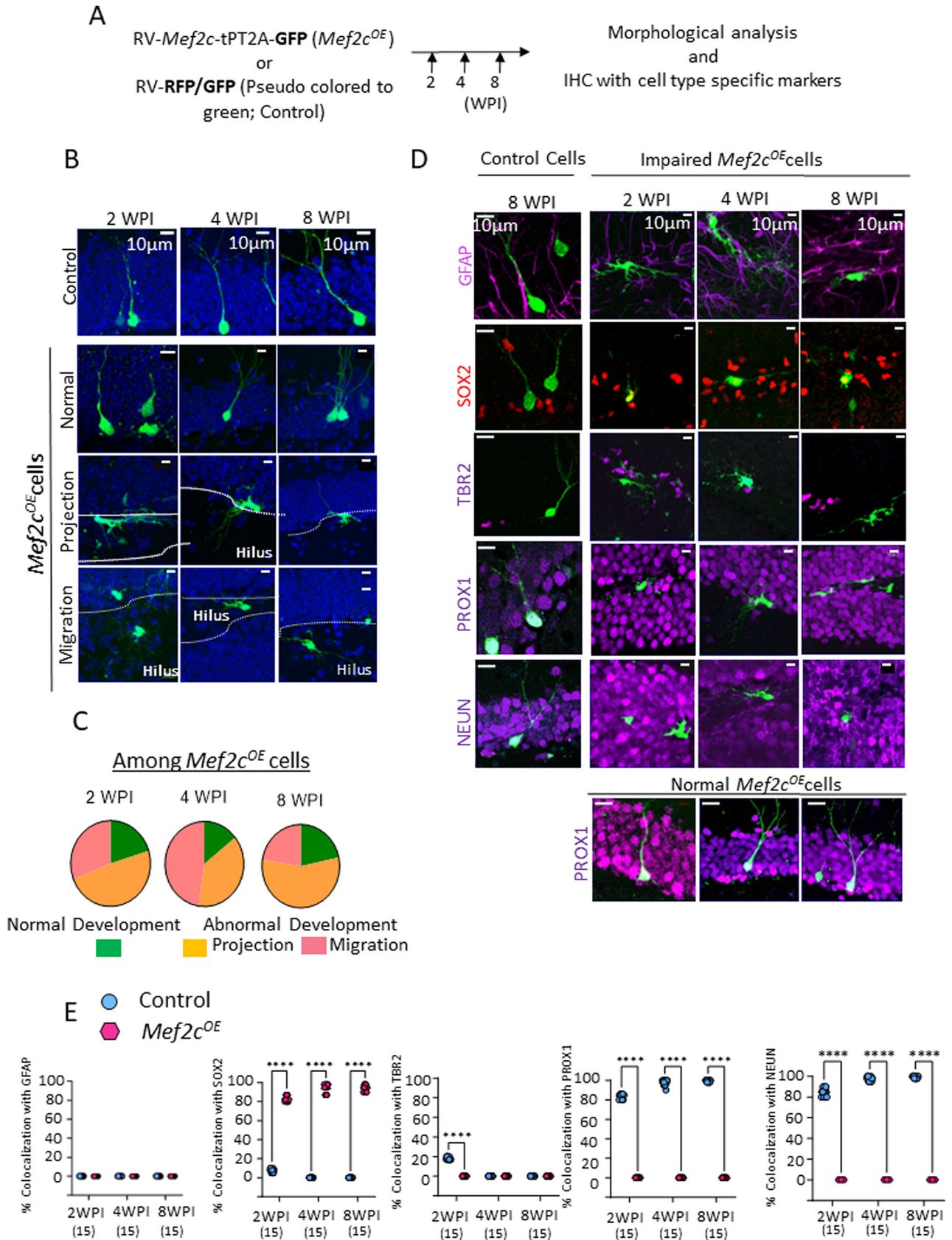
Figure 2. *Mef2c* overexpression halts neurogenesis. ***A***, Experimental scheme to examine the effects of *Mef2c* overexpression on the structure and state of abDGCs. ***B,C***, The majority of *Mef2c*^OE newborn cells (green) displayed impaired projection of processes and aberrant migration up to 8 weeks after birth. Cells (*n* = 50–100) from three mice were examined. ***D,E***, While a subset of *Mef2c*^OE cells differentiated into PROX1^+ DGCs, the majority of *Mef2c*^OE cells that showed impaired projection and migration expressed SOX2, but not neuronal or astrocyte lineage-specific markers, such as TBR2, NEUN, PROX1, or GFAP, respectively. In comparison, control or RV-GFP/RFP-injected mice, 2, 4, and 8 WPI DGCs properly differentiated into PROX1^+ and NEUN^+ DGCs. Representative images of eight WP WT DGCs co-localizing with just PROX1 and NEUN and not with other lineage-specific markers. Per marker, *n* = 15 cells from three mice were examined. This arrest of neurogenesis of *Mef2c*^OE cells at progenitor stages was sustained for at least 8 weeks after the birth of newborn cells. *Mef2c*^OE cells and WT cells are shown in green, and lineage-specific markers are shown in magenta or red (SOX2). Numbers in the parentheses represent cell numbers.
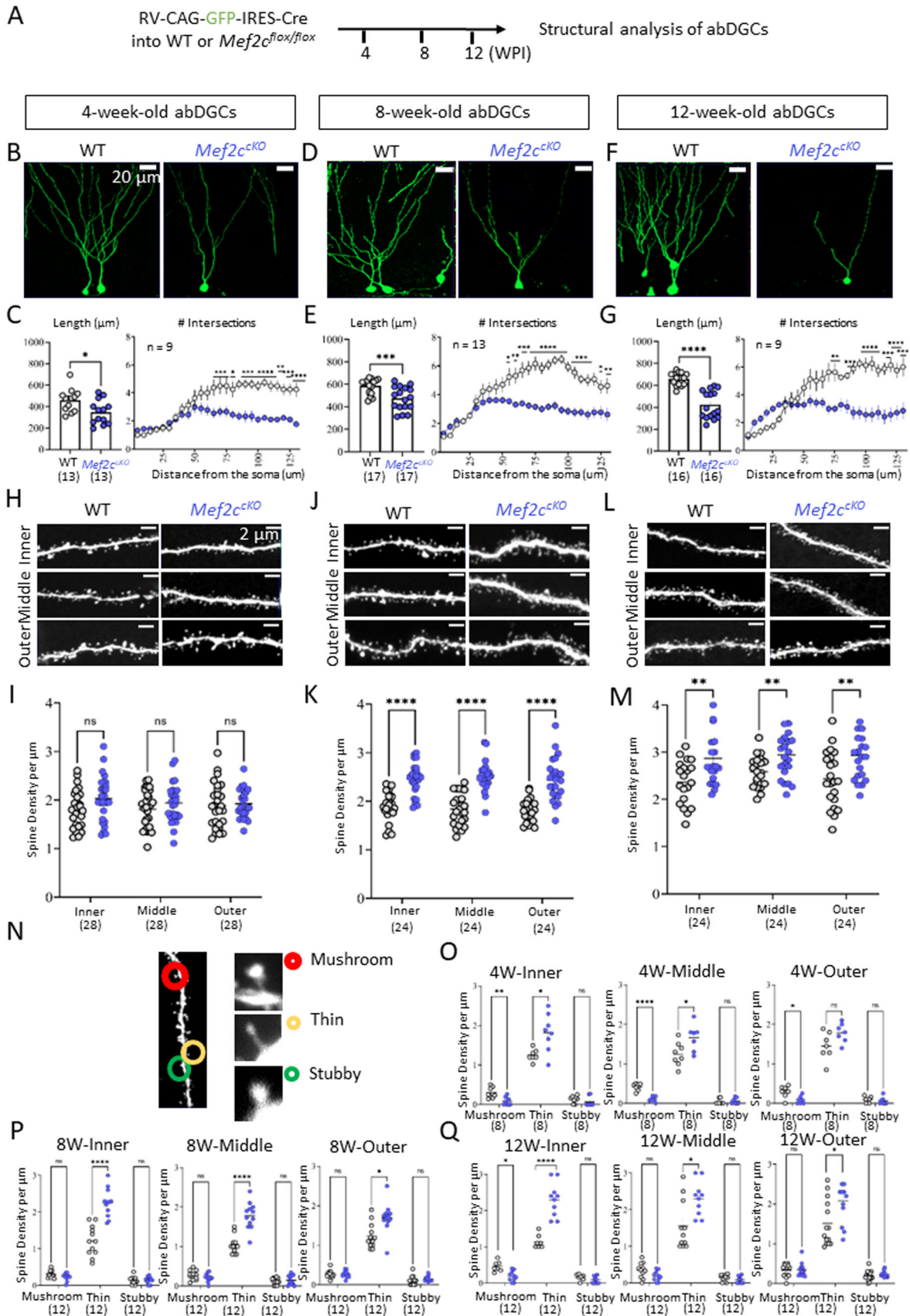
Figure 3. Continued.

in $Mef2c^{OE}$ cells was sustained up to 8 WPI, indicating that $Mef2c^{OE}$ sustained the expression of the neuronal progenitor marker, SOX2, irrespective of the ages of newborn cells (Fig. 2D,E). These results indicate that $Mef2c^{OE}$ did not simply delay neurogenesis, but it arrested newborn cells at the $SOX2^+$ neuronal progenitor stage and blocked neuronal differentiation of newborn cells.

MEF2C is required for the structural development of newborn neurons

To understand the essential role of MEF2C in the development of abDGCs, Mef2c was specifically deleted in abDGCs. We injected a RV that expresses both a CRE recombinase and GFP (RV-GFP-IRES-Cre) into the DG of $Mef2c^{flox/flox}$ and wild-type (WT) control mice and analyzed them at 4, 8, and 12 WPI (Fig. 3A). In mice in which Mef2c was conditionally knocked out ($Mef2c^{cKO}$), newborn cells successfully differentiated into abDGCs; however, the total dendritic length (Fig. 3B–G) and dendritic arborization (Fig. 3C,E,G) of $Mef2c^{cKO}$ abDGCs were significantly reduced in 4-, 8-, and 12-week-old abDGCs (total length, unpaired t tests, $p = 0.014$ at 4 WPI; $p = 0.0008$ at 8 WPI; and $p < 0.0001$ at 12 WPI; dendritic arborization, two-way ANOVA; main effect, genotype, $p < 0.0001$, $p = 0.0001$, and $p < 0.0001$ for 4, 8, and 12 WPI, respectively).

Next, we examined the function of Mef2c on dendritic spine formation. Because neurons from the lateral and medial entorhinal cortex (EC) and hilar mossy cells project onto the outer (distal), middle (medial), and inner (proximal) regions of dendrites of abDGCs (Amaral et al., 2007), spine densities of abDGCs were examined at the different segments of dendrites (Golub et al., 2015; Lee et al., 2019). Four-week-old $Mef2c^{cKO}$ abDGCs did not show any significant differences in spine density in any of the three dendritic segments (unpaired t tests; $p > 0.05$ at inner, middle, and outer segments; Fig. 3H,I); however, the spine densities in all three dendritic segments of abDGCs were significantly increased in 8- and 12-week-old $Mef2c^{cKO}$ abDGCs (Fig. 3J–M; 8 WPI, unpaired t tests, $p < 0.00001$ for all segments; 12 WPI, unpaired t test, $p = 0.004$ in inner, $p = 0.006$ in middle, and $p = 0.006$ in outer dendrites), suggesting a role of Mef2c in spine development at the later stages of neuronal development of abDGCs. We further analyzed the types of dendritic spines in $Mef2c^{cKO}$ abDGCs. The loss of Mef2c decreased the densities of mushroom spines in all three segments at 4 WPI, but the differences were not significant at later stages of development except in the proximal dendrites at 12 WPI (Fig. 3O; $p = 0.002$ for inner, $p = 0.00003$ for middle, and $p = 0.01$ for outer segments at 4 WPI). Interestingly, the densities of filopodial or thin spines instead increased at 8 WPI, and the increased densities of filopodia were sustained at 12 WPI of $Mef2c^{cKO}$ abDGCs. The increased densities of these thin spines were evident regardless of dendritic segment of abDGCs (Fig. 3N–Q; unpaired t tests; $p = 0.000002$,

inner and middle segments; $p = 0.0036$, outer segments at 8 WPI; $p = 0.000001$ inner segments; $p = 0.009$, middle segments; $p = 0.01$, outer segments at 12 WPI).

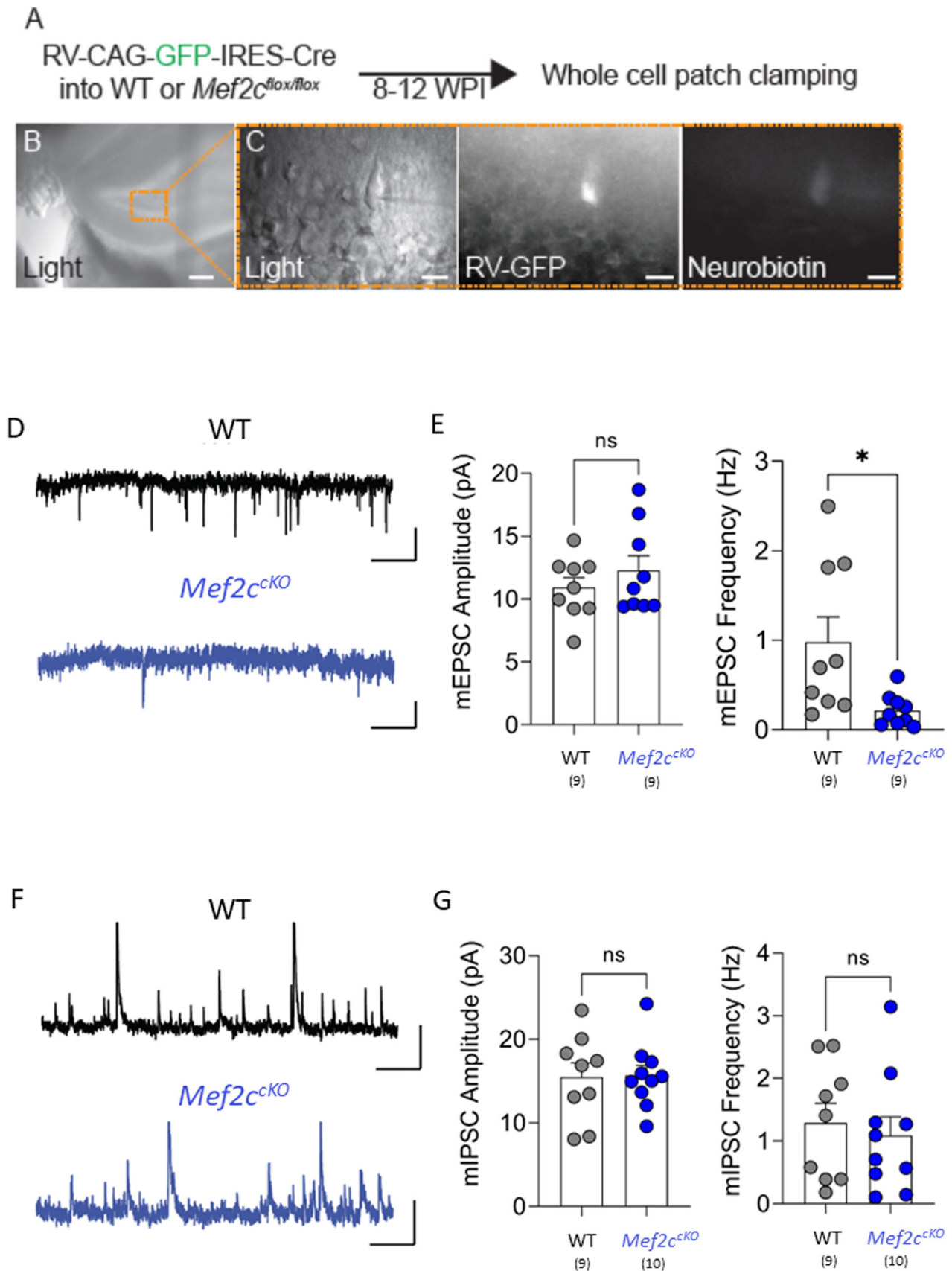## Mef2c deficiency leads to reduced synaptic transmission to abDGCs

To understand the impact of impaired spine formation on the synaptic transmission onto $Mef2c^{cKO}$ abDGCs, we performed ex vivo electrophysiology. WT and $Mef2c^{flox/flox}$ mice were injected with RV-CAG-GFP-IRES-Cre, and a whole-cell patch clamp was performed on abDGCs between 8 and 12 WPI (Fig. 4A–C). Compared to age-matched control abDGCs, the frequency, but not amplitude, of miniature excitatory postsynaptic currents (mEPSCs) was significantly reduced in $Mef2c^{cKO}$ abDGCs (unpaired t tests; $p = 0.0182$ for frequency and $p = 0.3532$ for amplitude) [Fig. 4D,E; $n = 9$ cells/group (6 mice/group)]; however, neither the frequency nor amplitude of miniature inhibitory postsynaptic currents (mIPSCs) were altered in $Mef2c^{cKO}$ abDGCs [unpaired t tests; $p = 0.6460$ for frequency and $p = 0.9341$ for amplitude; Fig. 4F,G; $n = 9$ cells/group (6 mice/group)]. These results show that Mef2c deletion specifically reduced excitatory synaptic transmission onto $Mef2c^{cKO}$ abDGCs.

The absence of Mef2c in abDGCs is sufficient for the expression of ASD behaviors

Consistent with an association between MEF2C and ASD, Mef2c heterozygote mice display ASD behaviors (Harrington et al., 2016; Anacker and Hen, 2017). Given the implication of MEF2C in ASD and the role of hippocampal neurogenesis in ASD behaviors, we investigated how an absence of Mef2c in abDGCs would affect cognitive and social behaviors, the latter being a prominent characteristic of ASD.

We generated double transgenic mice that harbor Ascl1-CreER and $Mef2c^{flox/flox}$ alleles, $Ascl1-CreER^{T2}$; $Mef2c^{flox/flox}$, which allowed us to delete Mef2c in abDGCs in a temporal-specific manner (Kim et al., 2007). $Mef2c^{flox/flox}$ littermates were used as controls (Fig. 5A). Consistently with a previous report (Kim et al., 2007), we confirmed that tamoxifen-mediated activation of CreER induced the expressions of EYFP in abDGCs when we tested with a separate cohort of Ascl1-CreERT2;ROSA26 reporter mice (Fig. 5B). Tamoxifen was injected into 6- to 8-week-old $Ascl1-CreER^{T2};Mef2c^{flox/flox}$ ($Mef2c^{cKO}$) and control mice, and then mice were subjected to three-chamber social interaction and social novelty tests 8–12 weeks after tamoxifen injection. Both control and $Mef2c^{cKO}$ did not show any side preference when objects were presented in both chambers (Fig. 5C,D). While control mice spent more time with live mice than with objects, $Mef2c^{cKO}$ mice displayed no preference for live mice over objects, showing comparable interaction times (Fig. 5E,F; two-way ANOVA, main effect: social objects, $p = 0.004$). Subsequently, the object was replaced with a novel mouse,

←

Figure 3. MEF2C is required for the structural and synaptic development of newborn neurons. **A**, Experimental design to delete Mef2c in hippocampal abDGCs and timeline of analysis. **B–G**, Specific deletion of Mef2c in abDGCs reduced the total dendritic lengths and arborization of 4-week-old (**B,C**, total dendritic length, $n = 13$; Sholl analysis, $n = 9$), 8-week-old (**D,E**, total dendritic length, $n = 16$; Sholl analysis, $n = 13$), and 12-week-old (**F,G**, total dendritic length, $n = 16$; Sholl analysis, $n = 9$) abDGCs. **H–M**, Specific deletion of Mef2c in abDGCs did not change dendritic spine densities in 4-week-old abDGCs (**I**, $n = 28$/group); however, dendritic spine densities of 8-week-old (**K**, $n = 24$/group) and 12-week-old (**M**, $n = 24$/group) $Mef2c^{cKO}$ abDGCs were significantly reduced regardless of the locations of the spines along the dendrite. **N**, Representative images showing different types of spines that include mushroom, thin, and stubby spines. **O**, Mef2c deficiency in abDGCs decreased and increased the densities of mushroom and thin spines of 4-week-old abDGCs, respectively, while those of stubby spines were unchanged ($n = 8$/group). **P,Q**, Both 8-week-old ($n = 12$/group) and 12-week-old ($n = 8$/group) $Mef2c^{cKO}$ abDGCs showed increased densities of thin spines along the dendrite. For Sholl analysis, two-way ANOVA with Bonferroni's multiple comparison tests. For the other experiments, Student's t test, $*p < 0.05$; $**p < 0.01$; $***p < 0.001$; $****p < 0.0001$. Numbers in the parentheses represent cell numbers. Data are represented as mean ± SEM.

Figure 4. *Mef2c* deficiency leads to reduced synaptic transmission onto abDGCs. *A*, Experimental design to delete *Mef2c* in abDGCs and perform whole-cell patch clamping. *B,C*, CCD Camera captured infrared (*B,C* left) and fluorescence (*C* middle with ET-GFP filter and *C* right with ET-DAPI filter) images showing the recorded abDGCs in the whole-cell recording. Scale bar = 200 μm (*B*) and 20 μm (*C*). *D,E*, mEPSC frequencies, but not amplitudes, of *Mef2c^{cKO}* abDGCs were significantly decreased in *Mef2c^{cKO}* abDGCs (n_l = 9 cells/group [6 mice/group]). *F,G*, The absence of *Mef2c* did not impact the frequencies or amplitudes of mIPSCs of abDGCs [n = 9–10 cells/group (6 mice/group)]. Numbers in the parentheses represent cell numbers. Data are represented as mean ± SEM. Student's *t* test, *$p < 0.05$.
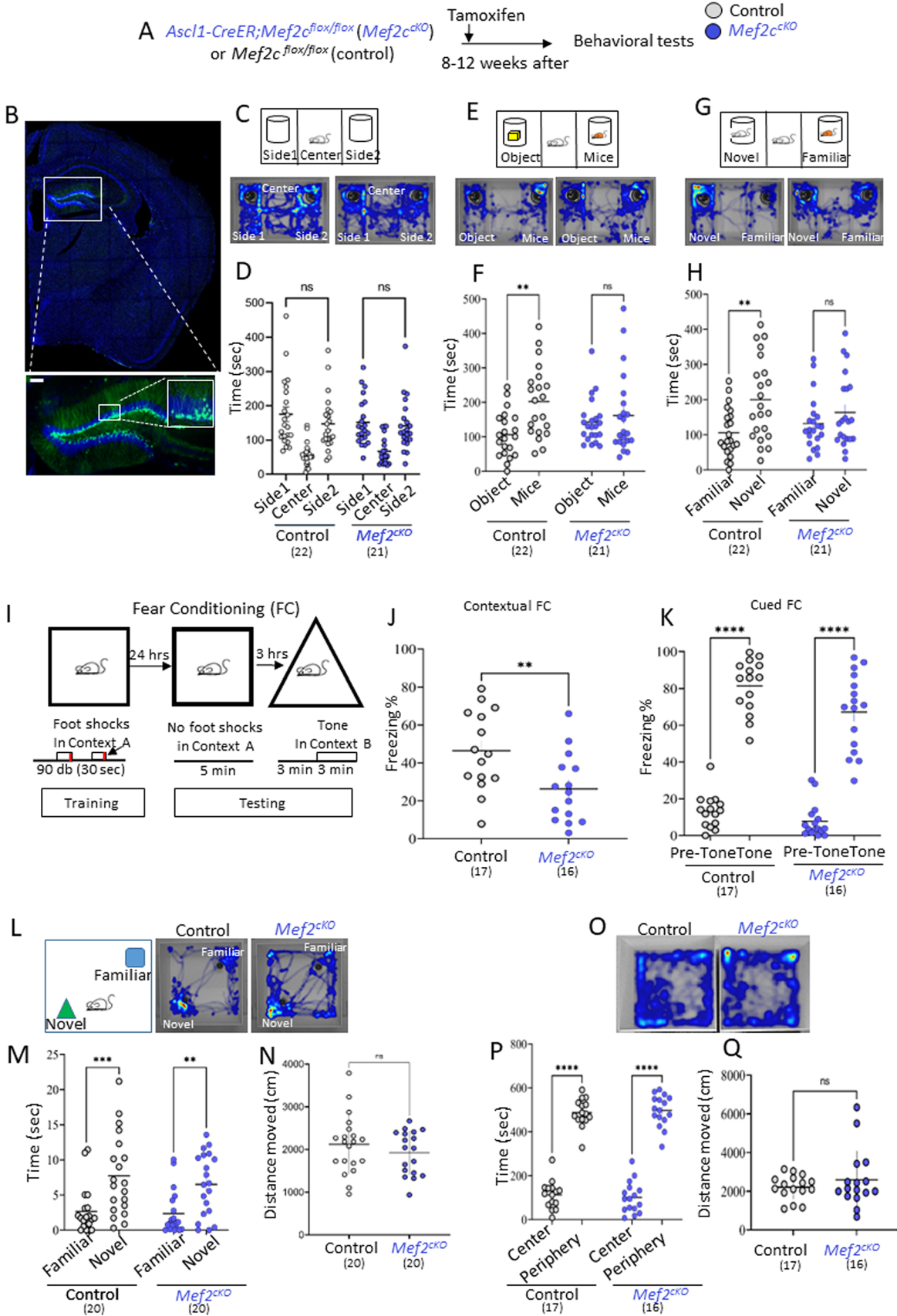
Figure 5. Continued.

and then mice were subject to interact with a novel mouse (that replaced the object) or a familiar mouse (the same that was used for the sociability test). As expected, control mice spent significantly more time with the novel mouse; however, $Mef2c^{cKO}$ mice did not show any preference for the novel mouse, and the interaction times of $Mef2c^{cKO}$ mice with familiar and novel mice were not significantly different (two-way ANOVA, main effect: social novelty, $p = 0.005$; Fig. 5G,H), indicating both sociability and social novelty discrimination deficits in $Mef2c^{cKO}$ mice.

Next, we tested the contextual and cued fear memory of $Mef2c^{cKO}$ mice. Mice were first trained to associate white noise with foot shocks in a specific context, and then we tested whether the context or tone could induce freezing behavior without the actual presentation of foot shocks (Fig. 5I). When mice were re-exposed to the same context where they had received the foot shock, $Mef2c^{cKO}$ mice showed significantly less freezing time compared to control mice (unpaired t test, $p = 0.009$; Fig. 5J). However, tone-induced freezing behavior did not show any significant difference compared to that of control mice (two-way ANOVA, main effect: genotype, $p < 0.0001$ for both control and $Mef2c^{cKO}$; Fig. 5K), indicating that $Mef2c^{cKO}$ in abDGCs led to deficits in the ability to associate to context. In the novel object recognition test, both control and $Mef2c^{cKO}$ mice spent more time with the novel object than with the familiar object, revealing comparable levels of discrimination ability (two-way ANOVA, main effect: genotype, $p = 0.0003$ for control and $p = 0.0031$ for $Mef2c^{cKO}$; Fig. 5L,M). The open field test showed that control and $Mef2c^{cKO}$ mice did not show any differences in time spent in the periphery and central zones (two-way ANOVA, main effect: genotype, $p < 0.0001$ for both control and $Mef2c^{cKO}$; Fig. 5O,P). During the behavior tests, $Mef2c^{cKO}$ mice did not show any differences in motility compared to control mice (Fig. 5N,Q).

Discussion

In this study, we showed how a transcriptional factor, $Mef2c$, regulates the development and synaptic connectivity of hippocampal newborn neurons, and how the altered structure of abDGCs, in turn, disrupts hippocampus-dependent physiology, function, and behavior. The $Mef2$ gene family has distinct temporal and spatial expression patterns in the developing and adult brains and plays a critical role in neuronal development (Dietrich, 2013). $Mef2c$ is highly expressed in the cortex, amygdala, and hippocampus, and it controls gene expression in an activity-dependent manner (Lyons et al., 2012; Dietrich, 2013; Assali et al., 2019; Chen et al., 2020a). In particular, $Mef2c$ has been recognized to play an important role in the context of synapse elimination, since $Mef2c$ deletion increases synaptic densities (Pfeiffer et al., 2010; Tsai et al., 2012; Hussaini et al., 2014). Interestingly, alterations in the chromosome containing $Mef2c$

loci and genetic deletion of $Mef2c$ have been associated with ASD, suggesting that synaptic and neuronal connectivity are key elements that determine autism pathobiology. Given that hippocampal neurogenesis is tightly regulated by activity and that disrupted hippocampal neurogenesis has often been associated with autism (Guo et al., 2011; Stephenson et al., 2011; Amiri et al., 2012; Hussaini et al., 2014; Haan et al., 2021; Gioia et al., 2022), it is reasonable to hypothesize that $Mef2c$ may play an important role in ASD-related behaviors by regulating hippocampal neurogenesis. Although the contribution of the entire $Mef2$ gene family to hippocampal neurogenesis has been addressed (Latchney et al., 2015), the specific role of $Mef2c$ in hippocampal neurogenesis, and its functional significance in physiology and behavior, has yet remained unanswered. Here, using conditional deletion of $Mef2c$ in hippocampal newborn neurons or abDGCs, we have demonstrated how $Mef2c$ impacts behavior by regulating the structural development, physiology, and function of abDGCs.

Hippocampal neurogenesis is sensitive to $Mef2c$ gene dosage
During hippocampal neurogenesis, $Mef2c$ expression was initially detected in a small population of SOX2$^+$ NSCs, gradually increased in DCX$^+$ neuroblasts/immature neurons, and was eventually maintained in DGCs. The specific overexpression ($Mef2c^{OE}$) and deletion ($Mef2c^{cKO}$) of $Mef2c$ in the lineage of newborn cells revealed the gene dosage sensitivity of hippocampal neurogenesis to $Mef2c$. Our virus-mediated gene delivery system predominantly infects and transduces $Mef2c$ in proliferating cells that subsequently give rise to abDGCs (Lee et al., 2019; Zhou et al., 2019; Zhang et al., 2020). $Mef2c^{OE}$ cells did not express neuronal lineage-specific markers but sustained the expression of SOX2, a marker for neural stem/progenitors (Suh et al., 2007), even at 8 weeks after birth, indicating that $Mef2c^{OE}$ maintained cells undifferentiated. This is reminiscent of the $Mef2c$ function as a cardiac stem cell factor, which has been used to produce undifferentiated cardiac stem cells (Ieda et al., 2010), suggesting that $Mef2c^{OE}$ keeps cells from differentiating. Moreover, $Mef2c^{OE}$ induced abnormal development of processes and aberrant migration, indicating that a higher level of $Mef2c$ not only stalled the progression of neurogenesis but also impaired structural development and migration of newborn cells. On the contrary, our retrovirus-mediated specific deletion of $Mef2c$ did not interfere with the neuronal commitment of NSCs. $Mef2c^{cKO}$ cells differentiated into abDGCs, expressing neuronal lineage-specific markers such as DCX, NEUN, and PROX1 (data not shown); however, $Mef2c^{cKO}$ impaired the arborization of abDGCs and abnormally increased spine density. Specifically, densities of thin spines or filopodia were significantly increased, while those of mushroom spines were relatively unaltered in $Mef2c^{cKO}$ abDGCs. The increased densities of filopodia may be attributed to the function of $Mef2c$ in synapse elimination as proposed

←

Figure 5. The absence of $Mef2c$ in abDGCs is sufficient for the expression of ASD-like behaviors. **A**, Experimental design to produce $Mef2c^{cKO}$ and to perform behavioral tests. **B**, Expression of EYFP in $Ascl1$-$CreER$; $Mef2c^{flox/flox}$; $Ai3^{flox/flox}$ showing that EYFP is expressed only in the hippocampal DGCs. **C,D**, Both control and $Mef2c^{cKO}$ had no bias towards any one side in the three-chamber sociability test. **E,F**, While control mice spent more time with live mice than objects, $Mef2c^{cKO}$ mice failed to display social interaction (control, $n = 22$; $Mef2c^{cKO}$, $n = 21$). **F,G**, Control mice spent more time with novel mice than familiar mice; however, $Mef2c^{cKO}$ mice displayed an impaired preference in social novelty recognition (control, $n = 22$; $Mef2c^{cKO}$, $n = 21$). **I–K**, $Mef2c^{cKO}$ mice showed deficits in contextual memory, showing decreased freezing time when they were re-exposed to the same context where they had received foot shocks (control, $n = 17$; $Mef2c^{cKO}$, $n = 16$). However, both $Mef2c^{cKO}$ and control mice showed comparable amounts of freezing time when the tone that had been associated with foot shocks was applied in a context that was not associated with the foot shocks (control, $n = 17$; $Mef2c^{cKO}$, $n = 16$). **L,M**, $Mef2c^{cKO}$ mice did not show any differences in recognition memory in the novel object recognition test compared to control mice (control, $n = 20$; $Mef2c^{cKO}$, $n = 20$). **O,P**, $Mef2c^{cKO}$ mice did not show any differences in preference between the center and peripheral zones compared to control mice (control, $n = 17$; $Mef2c^{cKO}$, $n = 16$). **N,Q**, Both control and $Mef2c^{cKO}$ moved comparable distances in the novel object recognition test and the open field test. Two-way ANOVA with Bonferroni's multiple comparison tests (**C,E,H,J,M**), Student's t test (**G,K**). *$p < 0.05$; **$p < 0.01$; ***$p < 0.001$; ****$p < 0.0001$. Numbers in the parentheses represent animal numbers. Data are represented as mean ± SEM.

previously (Pfeiffer et al., 2010; Tsai et al., 2012; Hussaini et al., 2014). This is also consistent with a previous observation that spine maturation is an activity-dependent process (Yasuda et al., 2021) and that lack of *Mef2c* may interfere with spine maturation or mushroom spine development. Collectively, our results revealed the requirement of a precise *Mef2c* dosage for tight control of multiple aspects of neurogenesis. The identification of molecular pathways that link *Mef2c* to activity-dependent synapse development of abDGCs and also a multiphoton-based in vivo microscopy approach to distinguish *Mef2c* function in spine elimination and formation or maturation from highly motile filopodia to stable spines are subjects of future research (Gonçalves et al., 2016b).

A cell-autonomous function of *Mef2c* in structure, physiology, and function of abDGCs

The function of *Mef2c* has been identified in multiple aspects such as neural stem cell differentiation (Lipton et al., 2009), activity-dependent survival (Mao et al., 1999), and maturation of newborn neurons, as well as synaptic transmission (Barbosa et al., 2008; Lipton et al., 2009; Harrington et al., 2016, 2020; Rajkovich et al., 2017). Several initial studies suggested a function of *Mef2c* in synapse elimination because an absence of *Mef2c* increased spine densities, and mEPSC frequency and intensities accordingly increased. Similarly, mEPSC frequencies of *Mef2c*-deficient DGCs in *hGFAP-Cre;Mef2$^{fl/fl}$* mice have also been shown to increase (Barbosa et al., 2008). Consistent with this result, our study showed increased dendritic spine densities in *Mef2c^{cKO}* abDGCs, revealing a critical role of *Mef2c* in structural development, as well as in determining the numbers and types of dendritic spines in abDGCs. However, *Mef2c^{cKO}* also decreased frequencies of mEPSCs of abDGCs. This difference in electrophysiological properties of *Mef2c^{cKO}* abDGCs may be due to the different contexts or experimental manipulations to delete *Mef2c* in DGCs. Since hGFAP-Cre induces the deletion of *Mef2c* in neural stem cells at early embryonic stages (Barbosa et al., 2008), it is expected that both pre- and postsynaptic neurons lack *Mef2c*. On the contrary, our viral or genetic manipulation resulted in the deletion of *Mef2c* exclusively in postsynaptic neurons. Indeed, the probability of neurotransmitter release increased at the pre-synaptic site in *hGFAP-Cre;Mef2$^{fl/fl}$* mice, indicating that both increased spine densities at the postsynaptic site and short-term synaptic activities at the pre-synaptic site contributed to increased synaptic transmission in *hGFAP-Cre;Mef2$^{fl/fl}$* mice. However, since our manipulation resulted in the deletion of *Mef2c* only in postsynaptic neurons, it is likely that intrinsic changes caused by the deletion of *Mef2c* led to reduced synaptic transmission onto abDGCs. Alternatively, this difference in mEPSC frequencies may reflect an environmental effect on *Mef2c*-deficient abDGCs. While all DGCs are expected to lack *Mef2c* in *hGFAP-Cre;Mef2c$^{fl/fl}$* mice, thereby *Mef2c*-deficient abDGCs are surrounded by *Mef2c*-deficient DGCs, our manipulations produced *Mef2c*-deficient abDGCs surrounded by WT DGCs. It is therefore possible that cell-non-autonomous effects may be reflected in the function of *Mef2c*-deficient cells in *hGFAP-Cre;Mef2c$^{fl/fl}$* mice. A previous study also suggested that environmental factors may influence the function of *Mef2c*-deficient cells. Genetic deletion of *Mef2c* in the majority of cortical excitatory neurons in *Emx-Cre;Mef2c$^{fl/fl}$* mice slightly decreased the frequencies and amplitudes of mEPSCs; however, mosaic deletion of *Mef2c* by infection with Cre-expressing adeno-associated virus in the same cortical excitatory neurons significantly increased both frequencies and amplitudes of mEPSCs (Harrington et al., 2016; Rajkovich et al., 2017). These results further suggest that both cell-autonomous and cell-non-autonomous effects need to be further investigated to gain a more complete understanding of the *Mef2c* function.

A role of abDGCs in social behavior

Patients harboring mutations in *MEF2C* have been linked to ASD. In addition, multiple animal models in which *Mef2c* is deleted have commonly displayed ASD-related behaviors. However, *Mef2c* mutations in the entire body (i.e., heterozygote for *Mef2c*) or vast areas of the brain (i.e., *Emx1-Cre* driven *Mef2c* deletion) hinder the field from identifying the precise brain area(s) that transmit *Mef2c* mutations to ASD-related behaviors. In this study, we identified hippocampal neurogenesis as a critical neural substrate that is necessary for *Mef2c*-dependent function and behavior. Hippocampal neurogenesis refers to the process by which new neurons are generated and incorporated into the pre-existing neural circuits. The precise regulation of hippocampal neurogenesis ensures tight control over the number of new neurons, as well as the structural development and neural circuit formation of newborn neurons. This controlled hippocampal neurogenesis provides ample plasticity, allowing the brain to exert cognitive functions and maintain emotional stability. Our study demonstrated that hippocampal neurogenesis has additional functions in social behavior. The specific deletion of *Mef2c* in abDGCs impaired social interactions, as well as the ability to recognize social novelty. This deficit in social behavior is one of the hallmarks manifested in ASD. This is interesting because a recent study proposed that the DG may be responsible for contextual novelty but that social novelty is attributed to CA2 (Hitti and Siegelbaum, 2014; Donegan et al., 2020; Chen et al., 2020b). However, ablation of hippocampal neurogenesis revealed its critical role in the maintenance of social behavior (Opendak et al., 2016). Moreover, deletions of many other ASD genes specifically in abDGCs commonly produced ASD-like social behaviors (Amiri et al., 2012; Guo et al., 2012; Chen et al., 2017b; Bicker et al., 2021; Kim et al., 2022), supporting a direct contribution of abDGCs to social behavior. It is intriguing that the recent discovery of direct projections of abDGCs to CA2 pyramidal neurons may explain the potential cooperative function of the DG to CA2 networks in social behaviors (Llorens-Martin et al., 2015; Whitebirch et al., 2022). Moreover, our observation that the conditional deletion of *Mef2c* in abDGCs disrupted contextual fear memory is in line with the recent reports on the role of *Mef2c* in cognitive function and resilience (Cole et al., 2012; Barker et al., 2021). Thus, these results collectively suggest that hippocampal neurogenesis is a critical neural substrate necessary for *Mef2c*-dependent social and cognitive behaviors.

References

Abbott LC, Nigussie F (2020) Adult neurogenesis in the mammalian dentate gyrus. Anat Histol Embryol 49:3–16.

Amaral DG, Scharfman HE, Lavenex P (2007) The dentate gyrus: fundamental neuroanatomical organization (dentate gyrus for dummies). Prog Brain Res 163:3–790.

Amiri A, Cho W, Zhou J, Birnbaum SG, Sinton CM, McKay RM, Parada LF (2012) Pten deletion in adult hippocampal neural stem/progenitor cells causes cellular abnormalities and alters neurogenesis. J Neurosci 32:5880–5890.

Anacker C, Hen R (2017) Adult hippocampal neurogenesis and cognitive flexibility—linking memory and mood. Nat Rev Neurosci 18:335–346.

Assali A, Harrington AJ, Cowan CW (2019) Emerging roles for MEF2 in brain development and mental disorders. Curr Opin Neurobiol 59:49–58.

Barbosa AC, Kim M-S, Ertunc M, Adachi M, Nelson ED, McAnally J, Richardson JA, Kavalali ET, Monteggia LM, Bassel-Duby R (2008) MEF2C, a transcription factor that facilitates learning and memory by negative regulation of synapse numbers and function. Proc Natl Acad Sci U S A 105:9391–9396.

Barker SJ, Raju RM, Milman NE, Wang J, Davila-Velderrain J, Gunter-Rahman F, Parro CC, Bozzelli PL, Abdurrob F, Abdelaal K (2021) MEF2 is a key regulator of cognitive potential and confers resilience to neurodegeneration. Sci Transl Med 13:eabd7695.

Bicker F, Nardi L, Maier J, Vasic V, Schmeisser MJ (2021) Criss-crossing autism spectrum disorder and adult neurogenesis. J Neurochem 159: 452–478.

Borlot F, Whitney R, Cohn RD, Weiss SK (2019) MEF2C-related epilepsy: delineating the phenotypic spectrum from a novel mutation and literature review. Seizure 67:86–90.

Bourgeron T (2015) From the genetic architecture to synaptic plasticity in autism spectrum disorder. Nat Rev Neurosci 16:551–563.

Castilla-Ortega E, Serrano A, Blanco E, Araos P, Suárez J, Pavón FJ, de Fonseca FR, Santín LJ (2016) A place for the hippocampus in the cocaine addiction circuit: potential roles for adult hippocampal neurogenesis. Neurosci Biobehav Rev 66:15–32.

Chen LF, Lyons MR, Liu F, Green MV, Hedrick NG, Williams AB, Narayanan A, Yasuda R, West AE (2020a) The NMDA receptor subunit GluN3A regulates synaptic activity-induced and myocyte enhancer factor 2C (MEF2C)-dependent transcription. J Biol Chem 295:8613–8627.

Chen S, et al. (2020b) A hypothalamic novelty signal modulates hippocampal memory. Nature 586:270–274.

Chen X, Gao B, Ponnusamy M, Lin Z, Liu J (2017a) MEF2 signaling and human diseases. Oncotarget 8:112152.

Chen Z, Li X, Zhou J, Yuan B, Yu B, Tong D, Cheng C, Shao Y, Xia S, Zhang R (2017b) Accumulated quiescent neural stem cells in adult hippocampus of the mouse model for the MECP2 duplication syndrome. Sci Rep 7:1–9.

Cole CJ, et al. (2012) MEF2 negatively regulates learning-induced structural plasticity and memory formation. Nat Neurosci 15:1255–1264.

Cope EC, Waters RC, Diethorn EJ, Pagliai KA, Dias CG, Tsuda M, Cameron HA, Gould E (2020) Adult-born neurons in the hippocampus are essential for social memory maintenance. eNeuro 7:ENEURO.0182-20.2020.

Cosgrove D, Whitton L, Fahey L, ÓBroin P, Donohoe G, Morris DW (2021) Genes influenced by MEF2C contribute to neurodevelopmental disease via gene expression changes that affect multiple types of cortical excitatory neurons. Hum Mol Genet 30:961–970.

Delorme R, Ey E, Toro R, Leboyer M, Gillberg C, Bourgeron T (2013) Progress toward treatments for synaptic defects in autism. Nat Med 19: 685–694.

Di Giorgio E, Franforte E, Cefalù S, Rossi S, Dei Tos AP, Brenca M, Polano M, Maestro R, Paluvai H, Picco R (2017) The co-existence of transcriptional activator and transcriptional repressor MEF2 complexes influences tumor aggressiveness. PLoS Genet 13:e1006752.

Dietrich J-B (2013) The MEF2 family and the brain: from molecules to memory. Cell Tissue Res 352:179–190.

Donegan ML, Stefanini F, Meira T, Gordon JA, Fusi S, Siegelbaum SA (2020) Coding of social novelty in the hippocampal CA2 region and its disruption and rescue in a 22q11. 2 microdeletion mouse model. Nat Neurosci 23:1365–1375.

Eisch AJ, Harburg GC (2006) Opiates, psychostimulants, and adult hippocampal neurogenesis: insights for addiction and stem cell biology. Hippocampus 16:271–286.

Ey E, Leblond CS, Bourgeron T (2011) Behavioral profiles of mouse models for autism spectrum disorders. Autism Res 4:5–16.

Flavell SW, Cowan CW, Kim T-K, Greer PL, Lin Y, Paradis S, Griffith EC, Hu LS, Chen C, Greenberg ME (2006) Activity-dependent regulation of MEF2 transcription factors suppresses excitatory synapse number. Science 311:1008–1012.

Gage FH (2019) Adult neurogenesis in mammals. Science 364:827–828.

Geschwind DH, Levitt P (2007) Autism spectrum disorders: developmental disconnection syndromes. Curr Opin Neurobiol 17:103–111.

Geschwind N (1965) Disconnexion syndromes in animals and man. Brain 88: 237–237.

Gioia R, Seri T, Diamanti T, Fimmanò S, Vitale M, Ahlenius H, Kokaia Z, Tirone F, Micheli L, Biagioni S (2022) Adult hippocampal neurogenesis and social behavioural deficits in the R451C neuroligin3 mouse model of autism are reverted by the antidepressant fluoxetine. J Neurochem 165:318–333.

Golub HM, Zhou QG, Zucker H, McMullen MR, Kokiko-Cochran ON, Ro EJ, Nagy LE, Suh H (2015) Chronic alcohol exposure is associated with decreased neurogenesis, aberrant integration of newborn neurons, and cognitive dysfunction in female mice. Alcohol Clin Exp Res 39:1967–1977.

Gonçalves JT, Schafer ST, Gage FH (2016a) Adult neurogenesis in the hippocampus: from stem cells to behavior. Cell 167:897–914.

Gonçalves JT, Bloyd CW, Shtrahman M, Johnston ST, Schafer ST, Parylak SL, Tran T, Chang T, Gage FH (2016b) In vivo imaging of dendritic pruning in dentate granule cells. Nat Neurosci 19:788–791.

Guo W, et al. (2011) Ablation of Fmrp in adult neural stem cells disrupts hippocampus-dependent learning. Nat Med 17:559–565.

Guo W, Murthy AC, Zhang L, Johnson EB, Schaller EG, Allan AM, Zhao X (2012) Inhibition of GSK3β improves hippocampus-dependent learning and rescues neurogenesis in a mouse model of fragile X syndrome. Hum Mol Genet 21:681–691.

Haan N, Westacott LJ, Carter J, Owen MJ, Gray WP, Hall J, Wilkinson LS (2021) Haploinsufficiency of the schizophrenia and autism risk gene Cyfip1 causes abnormal postnatal hippocampal neurogenesis through microglial and Arp2/3 mediated actin dependent mechanisms. Transl Psychiatry 11:313.

Harrington AJ, Raissi A, Rajkovich K, Berto S, Kumar J, Molinaro G, Raduazzo J, Guo Y, Loerwald K, Konopka G (2016) MEF2C regulates cortical inhibitory and excitatory synapses and behaviors relevant to neurodevelopmental disorders. Elife 5:e20059.

Harrington AJ, Bridges CM, Berto S, Blankenship K, Cho JY, Assali A, Siemsen BM, Moore HW, Tsvetkov E, Thielking A (2020) MEF2C hypofunction in neuronal and neuroimmune populations produces MEF2C haploinsufficiency syndrome–like behaviors in mice. Biol Psychiatry 88: 488–499.

Hitti FL, Siegelbaum SA (2014) The hippocampal CA2 region is essential for social memory. Nature 508:88–92.

Hong SI, Kang S, Chen JF, Choi DS (2019) Indirect medium spiny neurons in the dorsomedial striatum regulate ethanol-containing conditioned reward seeking. J Neurosci 39:7206–7217.

Hussaini SMQ, Choi C-I, Cho CH, Kim HJ, Jun H, Jang M-H (2014) Wnt signaling in neuropsychiatric disorders: ties with adult hippocampal neurogenesis and behavior. Neurosci Biobehav Rev 47:369–383.

Ieda M, Fu JD, Delgado-Olguin P, Vedantham V, Hayashi Y, Bruneau BG, Srivastava D (2010) Direct reprogramming of fibroblasts into functional cardiomyocytes by defined factors. Cell 142:375–386.

Kang S, Hong SI, Lee J, Peyton L, Baker M, Choi S, Kim H, Chang SY, Choi DS (2020) Activation of astrocytes in the dorsomedial striatum facilitates transition from habitual to goal-directed reward-seeking behavior. Biol Psychiatry 88:797–808.

Kim EJ, Leung CT, Reed RR, Johnson JE (2007) In vivo analysis of Ascl1 defined progenitors reveals distinct developmental dynamics during adult neurogenesis and gliogenesis. J Neurosci 27:12764–12774.

Kim H, Cho B, Park H, Kim J, Kim S, Shin J, Lengner CJ, Won K-J, Kim J (2022) Dormant state of quiescent neural stem cells links Shank3 mutation to autism development. Mol Psychiatry 27:2751–2765.

Lagace DC, Donovan MH, DeCarolis NA, Farnbauch LA, Malhotra S, Berton O, Nestler EJ, Krishnan V, Eisch AJ (2010) Adult hippocampal neurogenesis is functionally important for stress-induced social avoidance. Proc Natl Acad Sci U S A 107:4436–4441.

Latchney SE, Jiang Y, Petrik DP, Eisch AJ, Hsieh J (2015) Inducible knock-out of Mef2a,-c, and-d from nestin-expressing stem/progenitor cells and their progeny unexpectedly uncouples neurogenesis and dendritogenesis in vivo. FASEB J 29:5059–5071.

Le Meur N, Holder-Espinasse M, Jaillard S, Goldenberg A, Joriot S, Amati-Bonneau P, Guichet A, Barth M, Charollais A, Journel H (2010) MEF2C haploinsufficiency caused by either microdeletion of the 5q14. 3 region or mutation is responsible for severe mental retardation with stereotypic movements, epilepsy and/or cerebral malformations. J Med Genet 47:22–29.

Lee D, Krishnan B, Zhang H, Park HR, Ro EJ, Jung Y-N, Suh H (2019) Activity of hippocampal adult-born neurons regulates alcohol withdrawal seizures. JCI Insight 4:e128770.

Lipton SA, Li H, Zaremba JD, McKercher SR, Cui J, Kang Y-J, Nie Z, Soussou W, Talantova M, Okamoto S-I (2009) Autistic phenotype from MEF2C knock-out cells. Science 323:208–208.

Liu Z, Chen O, Wall JBJ, Zheng M, Zhou Y, Wang L, Ruth Vaseghi H, Qian L, Liu J (2017) Systematic comparison of 2A peptides for cloning multigenes in a polycistronic vector. Sci Rep 7:2193.

Llorens-Martin M, Jurado-Arjona J, Avila J, Hernandez F (2015) Novel connection between newborn granule neurons and the hippocampal CA2 field. Exp Neurol 263:285–292.

Lyons GE, Micales BK, Schwarz J, Martin J, Olson EN (1995) Expression of mef2 genes in the mouse central nervous system suggests a role in neuronal maturation. J Neurosci 15:5727–5738.

Lyons MR, Schwarz CM, West AE (2012) Members of the myocyte enhancer factor 2 transcription factor family differentially regulate Bdnf transcription in response to neuronal depolarization. J Neurosci 32:12780–12785.

Mao Z, Bonni A, Xia F, Nadal-Vicens M, Greenberg ME (1999) Neuronal activity-dependent cell survival mediated by transcription factor MEF2. Science 286:785–790.

Medavarapu S, Marella LL, Sangem A, Kairam R (2019) Where is the evidence? A narrative literature review of the treatment modalities for autism spectrum disorders. Cureus 11:e3901.

Mignone JL, Kukekov V, Chiang AS, Steindler D, Enikolopov G (2004) Neural stem and progenitor cells in nestin-GFP transgenic mice. J Comp Neurol 469:311–324.

Montagrin A, Saiote C, Schiller D (2018) The social hippocampus. Hippocampus 28:672–679.

Moyses-Oliveira M, Yadav R, Erdin S, Talkowski ME (2020) New gene discoveries highlight functional convergence in autism and related neurodevelopmental disorders. Curr Opin Genet Dev 65:195–206.

Opendak M, Offit L, Monari P, Schoenfeld TJ, Sonti AN, Cameron HA, Gould E (2016) Lasting adaptations in social behavior produced by social disruption and inhibition of adult neurogenesis. J Neurosci 36:7027–7038.

Oppenheim RW (2019) Adult hippocampal neurogenesis in mammals (and humans): the death of a central dogma in neuroscience and its replacement by a new dogma. Dev Neurobiol 79:268–280.

Paciorkowski AR, Traylor RN, Rosenfeld JA, Hoover JM, Harris CJ, Winter S, Lacassie Y, Bialer M, Lamb AN, Schultz RA (2013) MEF2C haploinsufficiency features consistent hyperkinesis, variable epilepsy, and has a role in dorsal and ventral neuronal developmental pathways. Neurogenetics 14:99–111.

Parikshak NN, Luo R, Zhang A, Won H, Lowe JK, Chandran V, Horvath S, Geschwind DH (2013) Integrative functional genomic analyses implicate specific molecular pathways and circuits in autism. Cell 155:1008–1021.

Pereira AHM, Cardoso AC, Consonni SR, Oliveira RR, Saito A, Vaggione MLB, Matos-Souza JR, Carazzolle MF, Gonçalves A, Fernandes JL (2020) MEF2C repressor variant deregulation leads to cell cycle re-entry and development of heart failure. EBioMedicine 51:102571.

Pfeiffer BE, Zang T, Wilkerson JR, Taniguchi M, Maksimova MA, Smith LN, Cowan CW, Huber KM (2010) Fragile X mental retardation protein is required for synapse elimination by the activity-dependent transcription factor MEF2. Neuron 66:191–197.

Rajkovich KE, Loerwald KW, Hale CF, Hess CT, Gibson JR, Huber KM (2017) Experience-dependent and differential regulation of local and long-range excitatory neocortical circuits by postsynaptic Mef2c. Neuron 93:48–56.

Rashid A, Cole C, Josselyn S (2014) Emerging roles for MEF2 transcription factors in memory. Genes Brain Behav 13:118–125.

Rocha H, Sampaio M, Rocha R, Fernandes S, Leao M (2016) MEF2C haploinsufficiency syndrome: report of a new MEF2C mutation and review. Eur J Med Genet 59:478–482.

Rubin RD, Watson PD, Duff MC, Cohen NJ (2014) The role of the hippocampus in flexible cognition and social behavior. Front Hum Neurosci 8:742.

Sahay A, Hen R (2007) Adult hippocampal neurogenesis in depression. Nat Neurosci 10:1110–1115.

Sebastian A, Hum NR, Morfin C, Murugesh DK, Loots GG (2018) Global gene expression analysis identifies Mef2c as a potential player in Wnt16-mediated transcriptional regulation. Gene 675:312–321.

Song J, Christian KM, Ming GL, Song H (2012) Modification of hippocampal circuitry by adult neurogenesis. Dev Neurobiol 72:1032–1043.

Song J, Olsen RH, Sun J, Ming G-L, Song H (2016) Neuronal circuitry mechanisms regulating adult mammalian neurogenesis. Cold Spring Harb Perspect Biol 8:a018937.

Stephenson DT, O'Neill SM, Narayan S, Tiwari A, Arnold E, Samaroo HD, Du F, Ring RH, Campbell B, Pletcher M (2011) Histopathologic characterization of the BTBR mouse model of autistic-like behavior reveals selective changes in neurodevelopmental proteins and adult hippocampal neurogenesis. Mol Autism 2:7.

Suh H, Consiglio A, Ray J, Sawai T, D'Amour KA and Gage FH (2007) In vivo fate analysis reveals the multipotent and self-renewal capacities of Sox2+ neural stem cells in the adult hippocampus. Cell Stem Cell 1:515–528.

Suh H, Deng W, Gage FH (2009) Signaling in adult neurogenesis. Annu Rev Cell Dev Biol 25:253–275.

Sun Y, Gao Y, Tidei JJ, Shen M, Hoang JT, Wagner DF, Zhao X (2019) Loss of MeCP2 in immature neurons leads to impaired network integration. Hum Mol Genet 28:245–257.

Toda T, Parylak SL, Linker SB, Gage FH (2019) The role of adult hippocampal neurogenesis in brain health and disease. Mol Psychiatry 24:67–87.

Tsai NP, Wilkerson JR, Guo W, Maksimova MA, DeMartino GN, Cowan CW, Huber KM (2012) Multiple autism-linked genes mediate synapse elimination via proteasomal degradation of a synaptic scaffold PSD-95. Cell 151:1581–1594.

Tu S, Akhtar MW, Escorihuela RM, Amador-Arjona A, Swarup V, Parker J, Zaremba JD, Holland T, Bansal N, Holohan DR (2017) Nitrosynapsin therapy for a mouse MEF2C haploinsufficiency model of human autism. Nat Commun 8:1488.

Voineagu I, Wang X, Johnston P, Lowe JK, Tian Y, Horvath S, Mill J, Cantor RM, Blencowe BJ, Geschwind DH (2011) Transcriptomic analysis of autistic brain reveals convergent molecular pathology. Nature 474:380–384.

Wan L, Liu X, Hu L, Chen H, Sun Y, Li Z, Wang Z, Lin Z, Zou L, Yang G (2021) Genotypes and phenotypes of MEF2C haploinsufficiency syndrome: new cases and novel point mutations. Front Pediatr 9:664449.

Wang J, Zhang Q, Chen Y, Yu S, Wu X, Bao X, Wen Y (2018) Novel MEF2C point mutations in Chinese patients with rett (− like) syndrome or nonsyndromic intellectual disability: insights into genotype-phenotype correlation. BMC Med Genet 19:191.

Whitebirch AC, LaFrancois JJ, Jain S, Leary P, Santoro B, Siegelbaum SA, Scharfman HE (2022) Enhanced excitability of the hippocampal CA2 region and its contribution to seizure activity in a mouse model of temporal lobe epilepsy. Neuron 110:3121–3138.e8.

Yasuda M, Nagappan-Chettiar S, Johnson-Venkatesh EM, Umemori H (2021) An activity-dependent determinant of synapse elimination in the mammalian brain. Neuron 109:1333–1349.e6.

Zhang H, Kim Y, Ro EJ, Ho C, Lee D, Trapp BD, Suh H (2020) Hippocampal neurogenesis and neural circuit formation in a cuprizone-induced multiple sclerosis mouse model. J Neurosci 40:447–458.

Zhang Z, Zhao Y (2022) Progress on the roles of MEF2C in neuropsychiatric diseases. Mol Brain 15:8.

Zhou QG, Nemes AD, Lee D, Ro EJ, Zhang J, Nowacki AS, Dymecki SM, Najm IM, Suh H (2019) Chemogenetic silencing of hippocampal neurons suppresses epileptic neural circuits. J Clin Invest 129:310–323.